Ewald et al. BMC Medical Genomics (2015) 8:60
DOI 10.1186/s12920-015-0133-x

BMC Medical Genomics

RESEARCH ARTICLE Open Access

Meta-analysis derived atopic dermatitis (MADAD) transcriptome defines a robust AD signature highlighting the involvement of atherosclerosis and lipid metabolism pathways

David A. Ewald[1,3,4], Dana Malajian[1,2,5], James G. Krueger[1], Christopher T. Workman[4], Tianjiao Wang[6], Suyan Tian[6], Thomas Litman[3], Emma Guttman-Yassky[1,2] and Mayte Suárez-Fariñas[1,2,7,8*]

Abstract

Background: Atopic dermatitis (AD) is a common inflammatory skin disease with limited treatment options. Several microarray experiments have been conducted on lesional/LS and non-lesional/NL AD skin to develop a genomic disease phenotype. Although these experiments have shed light on disease pathology, inter-study comparisons reveal large differences in resulting sets of differentially expressed genes (DEGs), limiting the utility of direct comparisons across studies.

Methods: We carried out a meta-analysis combining 4 published AD datasets to define a robust disease profile, termed meta-analysis derived AD (MADAD) transcriptome.

Results: This transcriptome enriches key AD pathways more than the individual studies, and associates AD with novel pathways, such as atherosclerosis signaling (IL-37, selectin E/SELE). We identified wide lipid abnormalities and, for the first time in vivo, correlated Th2 immune activation with downregulation of key epidermal lipids (FA2H, FAR2, ELOVL3), emphasizing the role of cytokines on the barrier disruption in AD. Key AD "classifier genes" discriminate lesional from nonlesional skin, and may evaluate therapeutic responses.

Conclusions: Our meta-analysis provides novel and powerful insights into AD disease pathology, and reinforces the concept of AD as a systemic disease.

Keywords: Atopic dermatitis, Meta-analysis, Transcriptome, Atherosclerosis, Expression analysis

Background

Atopic dermatitis (AD) is the most common inflammatory skin disease (4–7 % prevalence in adults, and ~15 % in children), with a large unmet need for safer and more effective treatments [1–7]. Immune and barrier abnormalities characterize AD, with Th2/Th22 cytokine activation, increased hyperplasia and significant decreases in differentiation markers. These observations have led to two competing pathogenic hypotheses [1, 8, 9], although recent studies characterizing AD primarily as an immune-driven disease have shown reversal of barrier defects following specific and non-specific therapeutic interventions [10–13].

Genomic expression profiling using gene-arrays and real time (RT)-PCR has been widely used to identify gene alterations in lesional (LS) and non-lesional (NL) AD compared to normal skin to better understand interactions between activation of cytokine pathways and epidermal abnormalities [6, 7, 10, 12, 14, 15]. Similar to other diseases, the AD phenotype/transcriptome can be defined genomically by differentially expressed genes (DEGs) between LS and NL skin [15]. A robust transcriptome was established as a powerful tool in identifying core psoriasis pathogenesis and evaluating the efficacy of targeted therapeutics at transcriptomic level

* Correspondence: farinam@rockefeller.edu
[1]The Laboratory for Investigative Dermatology, The Rockefeller University, New York, NY, USA
[2]Department of Dermatology, Icahn School of Medicine at Mount Sinai, New York, NY, USA
Full list of author information is available at the end of the article

BioMed Central

© 2015 Ewald et al. **Open Access** This article is distributed under the terms of the Creative Commons Attribution 4.0 International License (http://creativecommons.org/licenses/by/4.0/), which permits unrestricted use, distribution, and reproduction in any medium, provided you give appropriate credit to the original author(s) and the source, provide a link to the Creative Commons license, and indicate if changes were made. The Creative Commons Public Domain Dedication waiver (http://creativecommons.org/publicdomain/zero/1.0/) applies to the data made available in this article, unless otherwise stated.

[16, 17]. The high rates of placebo effect in AD patients contrasts with a worsening of disease phenotype at the transcriptomic level [10], reinforcing the importance of a robust disease transcriptome against which therapeutic effects can be evaluated [18]. Genomic profiling may also be used to predict therapeutic responses, as in juvenile idiopathic arthritis, in which profiling correctly predicted therapeutic responses at 6 months [19].

Nevertheless, high-throughput genomic analyses are vulnerable to multiple biases, including random noise, biological heterogeneity, and differences in experimental procedures (biopsies, hybridization, etc.), leading to remarkably little overlap between DEGs in similar scale studies [20–22]. A meta-analysis approach that combines microarray data from independent yet similarly designed studies allows one to overcome these variations, ultimately increasing the power and reproducibility of the transcriptome [23–25]. While several meta-analysis methods exist for combining microarray data from independent studies [26], the random-effects model (REM) has been established as one of the most suitable for heterogeneous studies [25, 27, 28].

We applied a REM meta-analysis model including 4 published AD microarray studies (including 97 samples; 54 LS and 43 NL; 41 paired) to determine core pathogenic elements and new disease associated genes [9, 10, 12, 15], resulting in the Meta-Analysis Derived AD (MADAD) disease transcriptome, a robust active disease signature of 595 DEGs, including 86 that were not previously detected by any individual study.

Methods

Sample collection

All samples were collected according to the Preferred Reporting Items for Systematic Reviews and Meta-Analyses (PRISMA) statement [29]. A total of 28 datasets were detected in Gene Expression Omnibus (GEO), but only datasets including LS and NL skin samples of AD patients were retained. Datasets run on platforms other than the HGU133Plus 2 chip, subject to treatments, or with non-randomly selected NL or LS samples (e.g. FLG homozygous/heterozygous loss of function mutation), and datasets without NL samples were excluded. When overlapping samples were found between datasets, only one copy was kept. Four microarray datasets satisfied the established criteria (GSE32924, GSE36842, GSE58558, GSE59294) [9, 10, 12, 15], including 97 samples (54 LS and 43 NL), which coincidently have been carried out by our group.

Pre-processing and expression analysis

Pre-processing and statistical analyses were performed using *R* and *Bioconductor* packages [30, 31]. Raw expression data were combined, summarized, and normalized using *GCRMA* [32]. Batch effects between datasets were adjusted for by the empirical Bayes method *ComBat/SVA* [32–35]. Agreement of the individual studies raw microarray data was estimated by the Integrated Correlation Coefficient Analysis, which produces the general Integrated Correlation Coefficient (ICC), representing agreement between studies, and can be interpreted in the same way as Pearson correlation coefficient. The ICC was used to eliminate background noise prior to the analysis, by excluding genes with incoherent behavior across studies [36].

For each study, estimation of differences in expression levels of LS vs NL skin was performed using the mixed-effect framework of the *limma* package.

Meta-analysis

The formal *random effects model (REM)*, described by Choi [27]. was applied to estimate the true effect size for each probe (see Additional file 1). These estimation and calculation steps were performed using the package *GeneMeta.* P-values were adjusted for multiple testing using the *Benjamini-Hochberg procedure* [37], with criteria for DEGs of absolute fold change ($|FCH| \geq 2.0$ and a false discovery rate (FDR) ≤ 0.05.

Post-processing

The MADAD transcriptome was subject to multiple downstream analysis methods. Integration-driven discovery/IDD-DEGs were defined as those not identified in any of the included studies. To explore functional annotations, overrepresentation analysis was carried out for BP GO-terms and KEGG pathways (both in DAVID) [38], Ingenuity Pathways (*IPA* – www.ingenuity.com, as described) [25], and on previously reported gene-sets [39].

The normalized LS and NL expression data were subject to Weighted Gene Co-Expression Networks Analysis (WGCNA) to detect clusters (modules) of correlated genes and respective hub genes [40]. These modules were subject to trait correlation and corresponding gene-set overrepresentation analysis.

Meta Threshold Gradient Directed Regularization (MTGDR) method [41, 42] was used to select disease-associated genes while allowing for varied estimates of those genes across different experiments, as previously published [41, 42].

Primers and probes were designed for RT-PCR as previously described (see Additional file 1 and Additional file 2) [43]. *Ribosomal protein, large, P0*/RPLP0 normalized RT-PCR expression data was analyzed using a mixed-effect framework after log2-transformation.

Lipid metabolism genes were defined as genes related to one of the four groups: *Ceramides*, *Free Fatty Acids*, *Sphingolipids*, and *Cholesteryl Esters* in the Gene Cards database (www.genecards.org). We included all genes with

a relevance score ≥ 10 [44, 45]. Pairwise Pearson correlations were calculated between the gene and patient specific deregulations. Multivariate correlations between sets of genes were calculated making use of the gene set specific μ-scores calculated by the *muStat* package [46].

Results

Data collection

Two major repositories (GEO Omnibus and ArrayExpress) were queried to identify studies with expression profiles of LS and NL punch biopsies from AD patients. Four studies (GSE59294, GSE58558, GSE36842, GSE32924; including 97 samples, with 54 LS and 43 NL, 41 paired) met all inclusion criteria following the PRISMA guidelines (see Methods, Additional file 3: Figure E1 and Additional file 4: Table E1) [9, 10, 12, 15]. We only used data from chronic lesions in the analysis. No significant differences in disease severity (as measured by Scoring of AD/SCORAD and Eczema Area and Severity/EASI indices) or IgE levels were found across patients who all had moderate-to-severe AD (SCORAD > 25; EASI > 12).

Meta-analysis framework

The Venn diagram in Fig. 1a represents the overlap of DEGs identified by the individual studies, including 25 consensus DEGs (see Additional file 5: Table E2). Besides inter-study variation, sources of inconsistency in DEGs include choice of model, annotation, cut-off, and non-uniform pre-processing steps [47]. To combine results of individual studies and to aggregate robust DEGs with reliable effect sizes, we chose a meta-analysis approach [21, 27].

To address these sources of inconsistency, we applied a uniform pre-processing pipeline to the combined datasets, incorporating noise reduction techniques as proposed [23, 25, 36, 47] (see Methods, Additional file 3: Figure E1C, and Additional file 1). This pre-processing increased the average of the pairwise maximum canonical

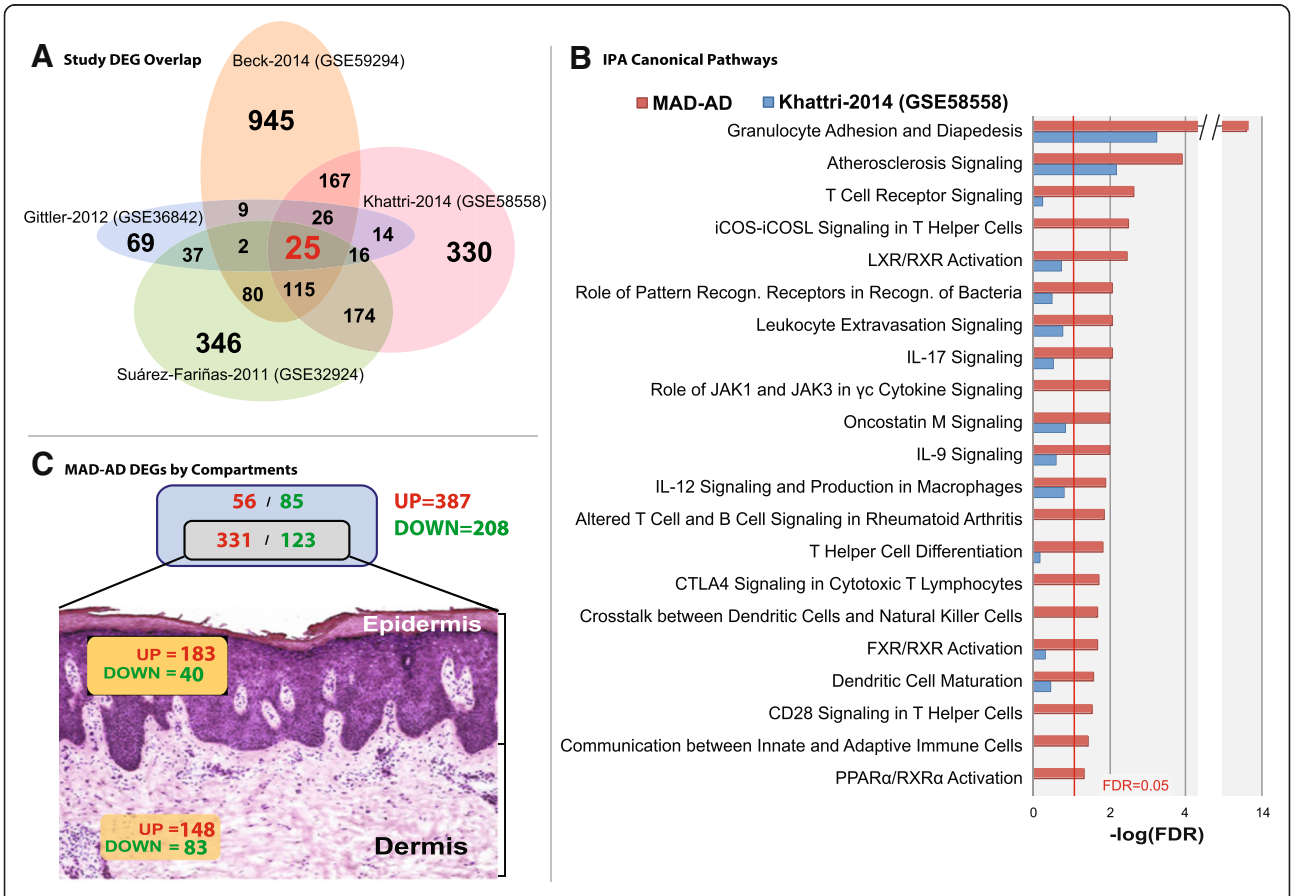

Fig. 1 a Approximate area proportional Venn diagram with overlaps of the differentially expressed genes of the four individually analyzed datasets under the same threshold (|FCH| ≥ 2, FDR ≤ 0.05). **b** Ingenuity Canonical Pathway overrepresentations compared between this MADAD transcriptome and the included dataset from Khattri et al. 2014 (GSE58558). The bars represent −log10 transformed Benjamini-Hochberg adjusted p-values termed −log(FDR), and the red threshold line indicates the FDR ≤ 0.05 cut-off. **c** Cutaneous localization of the MADAD transcriptome as compared to the epidermis and dermis related genes defined by Esaki et al. [63]

correlations between each pair of studies from 0.76 to 0.85.

To combine heterogeneous effect sizes across studies, a random effects model/REM was chosen over fixed effects model. The use of REM is supported by the sample distribution of the Cochran's Q statistic [27], which departs substantially from the theoretical χ^2_3-distribution under the assumption of homogeneity of study effects. Furthermore, a Kolmogorov-Smirnov-test also rejected the equality of these two distributions ($p = 2.22^{-15}$; D = 0.235) (Additional file 6: Figure E2).

The Meta-analysis-derived AD (MADAD) transcriptome

Applying the meta-analysis approach to 4 studies and 97 samples, we identified a set of 595 DEGs (387 up- and 208 downregulated) using the classical $|FCH| \geq 2$ and $FDR \leq 0.05$ criteria, representing a robust profile defined as the meta-analysis derived AD (MADAD) transcriptome (see Additional file 7: Table E3 for the entire MADAD DEGs list). Among the highest dysregulated genes are key AD genes, including markers of general inflammation (MMP12), specific T helper activation (e.g. Th2/CCL18, Th1/IFN/CXCL10, Th17/PI3/elafin, Th17/Th22 S100A7/A8/A9), and markers of epidermal proliferation (KRT16, Mki67).

To show the robustness of the MADAD transcriptome versus a single study, we conducted an over-representation analysis (see Methods) of ingenuity canonical pathways (IPA) and of previously published immune and barrier gene-sets [12, 48]. Figure 1b illustrates the comparison of the largest available' dataset (Khattri 2014 – GSE58558) and the MADAD transcriptome; similar results were obtained for the other three included datasets. Overall, the MADAD yields a more significant over-representation of key immune pathways, such as *Granulocyte Adhesion and Diapedesis, T Cell Receptor Signaling and differentiation*, *iCOS-iCOSL Signaling*, and *IL-12, IL-17,* and *IL-9 signaling*. Innate pathways (e.g. *Role of Pattern Recognition Receptors in Recognition of Bacteria*), which are associated with AD [49, 50], were also represented (Fig. 1b and Additional file 8: Tables E4 and Additional file 9: Table E5). Interestingly, *Atherosclerosis Signaling* was the second highest IPA pathway, and includes genes previously associated with vascular inflammation, such as IL-37, SERPINA1, S100A8, selectin E/SELE, lipoprotein lipase/LPL, and MMP1/3/9 [51–62]. An equivalent analysis of previously reported immune and barrier gene-sets [12] (Additional file 10: Figure E3A) similarly showed increased sensitivity and representation in the MADAD transcriptome compared to the largest data set, including IFNα, IL-4, immune genes, cytokine-treated keratinocytes and epidermal differentiation gene subsets (Additional file 10: Figure E3A). Thus, the MADAD transcriptome provides a more robust AD-specific signal, consistent with known disease pathology.

Comparison of the MADAD transcriptome to the recently described epidermal and dermal layer-specific transcriptomes linked 223 and 231 DEGs to the epidermis and dermis, respectively (Fig. 1c, Additional file 7: Table E3) [63]. Of these, 55.3 % of the upregulated genes were epidermal, whereas 67.5 % of the downregulated genes were dermal ($P = 2.6 \times 10^{-5}$, Fisher's exact test), as has been previously noted [63].

Of the top 25 up-regulated MADAD DEGs, 17 encode epidermal components, including key antimicrobial genes (DEFB4A, PI3/elafin, S100A9) (Additional file 7: Table E3). Top 25 up-regulated dermal genes include those related to collagen production (COL4A4, COL6A5) and inflammation (GZMB, OASL) [64, 65]. Among top down-regulated epidermal genes are structural/lipid-related genes (LEP, FABP7, ELOVL3), and genes linked to epidermal differentiation (CLDN8) [66–68]. Several genes associated with the pathogenesis of AD (e.g. IL-22, OX40L and TSLP) and reported in the layer-specific AD transcriptomes [63] were not detected in the MADAD transcriptome, most likely due to low expression levels of cytokines on whole tissue microarrays, a known limitation of microarrays [24, 69], that cannot be overcome by the meta-analysis approach.

Integration-Driven Discovery Genes in the MADAD transcriptome

The MADAD comprises a subset of IDD-DEGs, which were not detected by any of the individual datasets using identical cutoffs [9, 10, 12, 15]. These 86 IDD-DEGs consist of 45 up- and 41 downregulated genes (Table 1). Using IPA and GOterm overrepresentation analyses on the IDD-DEGs, we found in addition to the expected inflammatory processes (e.g. Chemokine Signaling), several pathways related to lipid and fatty acid metabolic processes (Additional file 10: Figure E3B, Additional file 11: Table E6).

We further validated, using RT-PCR, several IDD-DEGs and top MADAD DEGs with plausible biologic relevance to AD, including immune (CCL8, CD1E, IL-37, IL-36G), structural (AQP5, a water channel) and lipid (FAR2, ELOVL3, FA2H) genes, which encode enzymes involved in fatty acid and ceramide metabolism (Fig. 2a). Immune-related genes (e.g. CCL8, LCP2, CD1E) and IL-36G, which was recently associated with psoriasis pathogenesis [70], were increased in AD LS skin. The only gene that showed increased expression in NL vs LS skin was IL-37, a negative immune regulator [71], consistent with past reports [72]. All structural and lipid metabolism genes showed downregulation in LS AD skin ($P \leq 0.05$ for all), reinforcing the role of lipids and water channels in preserving barrier function in AD [73, 74].

Table 1 Integration-Driven Discovery (IDD) Genes in the MADAD transcriptome, with indication of compartmental allocation as defined by Esaki et al. [63]

Symbol	Description	logFC	FC	Layer
Up				
COL6A6	collagen, type VI, alpha 6	2,08	4,22	D
CD1B	CD1b molecule	1,84	3,57	D
SPRR1B	small proline-rich protein 1B	1,68	3,20	E
CCL22	chemokine (C-C motif) ligand 22	1,65	3,13	D
MMP9	matrix metallopeptidase 9 (gelatinase B, 92 kDa gelatinase, 92 kDa type IV collagenase)	1,51	2,84	D
IL13RA2	interleukin 13 receptor, alpha 2	1,46	2,74	D
CCL26	chemokine (C-C motif) ligand 26	1,37	2,59	D
SASH3	SAM and SH3 domain containing 3	1,35	2,56	D
IL36RN	interleukin 36 receptor antagonist	1,35	2,55	E
CCL13	chemokine (C-C motif) ligand 13	1,27	2,41	D
KIAA1644	KIAA1644	1,26	2,39	D
IL12RB1	interleukin 12 receptor, beta 1	1,23	2,34	D
XCL2	chemokine (C motif) ligand 2	1,21	2,31	D
CCL5	chemokine (C-C motif) ligand 5	1,21	2,31	D
ADAMDEC1	ADAM-like, decysin 1	1,19	2,29	D
TIFAB	TRAF-interacting protein with forkhead-associated domain, family member B	1,18	2,27	D
P2RY1	purinergic receptor P2Y, G-protein coupled, 1	1,16	2,23	E
PIK3CG	phosphatidylinositol-4,5-bisphosphate 3-kinase, catalytic subunit gamma	1,15	2,22	D
FAM124B	family with sequence similarity 124B	1,14	2,21	D
SLAMF8	SLAM family member 8	1,12	2,18	D
CXADR	coxsackie virus and adenovirus receptor	1,12	2,17	E
GPSM3	G-protein signaling modulator 3	1,11	2,16	D
HCK	hemopoietic cell kinase	1,09	2,13	D
LOC100288860	uncharacterized LOC100288860	1,09	2,12	E
MMP3	matrix metallopeptidase 3 (stromelysin 1, progelatinase)	1,08	2,11	D
CD1E	CD1e molecule	1,07	2,10	D
KLRK1	killer cell lectin-like receptor subfamily K, member 1	1,06	2,09	D
GBP1	guanylate binding protein 1, interferon-inducible	1,06	2,09	
IL23A	interleukin 23, alpha subunit p19	1,05	2,08	D
LYN	v-yes-1 Yamaguchi sarcoma viral related oncogene homolog	1,05	2,07	D
C5orf20	chromosome 5 open reading frame 20	1,05	2,06	D
CCL8	chemokine (C-C motif) ligand 8	1,04	2,06	D
RELB	v-rel avian reticuloendotheliosis viral oncogene homolog B	1,04	2,06	
ACPP	acid phosphatase, prostate	1,03	2,05	E
TRAT1	T cell receptor associated transmembrane adaptor 1	1,03	2,04	D
PTX3	pentraxin 3, long	1,03	2,04	D
CD48	CD48 molecule	1,03	2,04	D
FPR3	formyl peptide receptor 3	1,02	2,03	D
TGM3	transglutaminase 3	1,02	2,03	E
CXCL11	chemokine (C-X-C motif) ligand 11	1,02	2,03	
MAP4K1	mitogen-activated protein kinase kinase kinase kinase 1	1,02	2,02	D

Table 1 Integration-Driven Discovery (IDD) Genes in the MADAD transcriptome, with indication of compartmental allocation as defined by Esaki et al. [63] *(Continued)*

CD6	CD6 molecule	1,02	2,02	D
SELPLG	selectin P ligand	1,01	2,02	D
ZC3H12D	zinc finger CCCH-type containing 12D	1,01	2,01	D
C15orf48	chromosome 15 open reading frame 48	1,00	2,00	E
Down				
PM20D1	peptidase M20 domain containing 1	−2,63	−6,19	
KRT79	keratin 79	−2,04	−4,13	
GAL	galanin/GMAP prepropeptide	−2,02	−4,06	
ELOVL3	ELOVL fatty acid elongase 3	−1,71	−3,26	
CYP4F8	cytochrome P450, family 4, subfamily F, polypeptide 8	−1,64	−3,11	
HAO2	hydroxyacid oxidase 2 (long chain)	−1,63	−3,10	
FADS2	fatty acid desaturase 2	−1,49	−2,80	
ANGPTL7	angiopoietin-like 7	−1,40	−2,63	D
CUX2	cut-like homeobox 2	−1,36	−2,56	
PON3	paraoxonase 3	−1,35	−2,55	E
SGK2	serum/glucocorticoid regulated kinase 2	−1,32	−2,50	
MSMB	microseminoprotein, beta-	−1,31	−2,47	E
FADS1	fatty acid desaturase 1	−1,30	−2,46	D
BPY2	basic charge, Y-linked, 2	−1,29	−2,45	
FAR2	fatty acyl CoA reductase 2	−1,29	−2,44	D
MUC7	mucin 7, secreted	−1,23	−2,35	
FA2H	fatty acid 2-hydroxylase	−1,20	−2,30	
ABHD12B	abhydrolase domain containing 12B	−1,18	−2,27	E
PNPLA3	patatin-like phospholipase domain containing 3	−1,18	−2,27	E
ACOX2	acyl-CoA oxidase 2, branched chain	−1,11	−2,16	D
PSORS1C2	psoriasis susceptibility 1 candidate 2	−1,10	−2,15	E
KRT19	keratin 19	−1,08	−2,11	
ATP6V1B1	ATPase, H+ transporting, lysosomal 56/58 kDa, V1 subunit B1	−1,07	−2,10	
SCGB2B2	secretoglobin, family 2B, member 2	−1,07	−2,09	
MOGAT1	monoacylglycerol O-acyltransferase 1	−1,07	−2,09	
NSUN7	NOP2/Sun domain family, member 7	−1,07	−2,09	E
COCH	cochlin	−1,05	−2,07	E
IL20RA	interleukin 20 receptor, alpha	−1,05	−2,07	E
SEMA3B	sema domain, immunoglobulin domain (Ig), short basic domain, secreted, (semaphorin) 3B	−1,03	−2,05	D
RHPN2	rhophilin, Rho GTPase binding protein 2	−1,03	−2,05	
AWAT1	acyl-CoA wax alcohol acyltransferase 1	−1,03	−2,04	
TMC4	transmembrane channel-like 4	−1,03	−2,04	
GPRC5A	G protein-coupled receptor, class C, group 5, member A	−1,02	−2,03	
TRHDE-AS1	TRHDE antisense RNA 1	−1,02	−2,03	
AQP5	aquaporin 5	−1,02	−2,03	
LINC00663	long intergenic non-protein coding RNA 663	−1,02	−2,02	
ZNF471	zinc finger protein 471	−1,01	−2,02	

Table 1 Integration-Driven Discovery (IDD) Genes in the MADAD transcriptome, with indication of compartmental allocation as defined by Esaki et al. [63] *(Continued)*

CYP2J2	cytochrome P450, family 2, subfamily J, polypeptide 2	−1,01	−2,02	E
MEGF10	multiple EGF-like-domains 10	−1,01	−2,01	
FAXDC2	fatty acid hydroxylase domain containing 2	−1,00	−2,01	D
SLC13A2	solute carrier family 13 (sodium-dependent dicarboxylate transporter), member 2	−1,00	−2,01	

Suppression of lipid-related genes is coupled to increased Th2 activation

While we have previously shown inverse correlations between immune activation and terminal differentiation genes in AD lesions [11, 15], the relationship between immune activation and lipid metabolism genes has not been assessed in skin.

We thus investigated the relationship between expression of Th2-specific and epidermal lipid metabolism genes in the MADAD transcriptome. First we performed an unbiased database search for lipid related terms (see Methods) and chose genes with highest relevance scores. The correlation structure between lipid metabolism and immune genes in LS and NL skin is shown in Fig. 2b.

Unsupervised clustering identified two main sub-clusters in the Th2 gene-set and three main sub-clusters in the lipid metabolism gene-set. Cluster 3 consists only of SPTLC2, the only lipid metabolism gene with up-regulated expression in the MADAD transcriptome. This gene encodes serine palmitoyltransferase (SPT), a rate-limiting enzyme in sphingomyelin synthesis, whose elevated expression has been associated with increased barrier defects, including in AD [75–77].

Multivariate u-statistics correlate the dysregulation of immune and lipid metabolism genes [46]. Overall, an inverse correlation of −0.46 ($p = 0.003$) was obtained between Th2 and lipid subsets, supporting a proposed model of Th2 cytokine effects on lipid suppression [78]. Among Th2 genes, cluster 1 showed the highest negative correlation with lipid metabolism genes (−0.49; $p = 0.001$), and includes key AD genes (CCL22, IL-7R, and IL-4R) [63, 79–81]. Targeting IL-4R shows promise in early clinical trials as a possible therapeutic target for moderate-to-severe AD, and is now in phase 3 clinical trials for this disease (NCT02277743) [10, 18].

Weighted gene co-expression network analysis

Weighted gene co-expression network analysis (WGCNA) offers insights into disease pathogenesis by studying weighted co-expression of genes within tissue samples [40]. This technique requires a large sample size [40, 82], which we were able to apply here for the first time in AD (see Methods).

Using WGCNA, 21 distinct sub-networks were identified, and each was correlated with age, IgE level, and disease severity (measured by Scoring of Atopic Dermatitis/SCORAD) index (Fig. 3a-b, Additional file 12: Tables E7 and Additional file 13: Table E8). In LS skin, several networks showed significant positive correlations with SCORAD, including viral (M13) and innate immune response processes (M17), emphasizing cutaneous immune reactions to viral and/bacterial pathogens in LS AD skin. Proliferation and epidermal processes were also correlated with SCORAD (M10, M11), with a trend for negative correlations between SCORAD and structural epidermal modules (M4, M12). In NL skin, immune-related networks such as cytokine receptor signaling pathway and innate immune response modules (M4, M2) [63, 83] were also positively correlated with SCORAD, while extracellular matrix (ECM) organization (M10) and ECM-receptor interaction (M9) modules were negatively correlated (Fig. 3b). Interestingly, a trend for a positive correlation was observed between SCORAD and *Staphylococcus aureus* (*S.aureus*) infection in NL skin (M8), with possible clinical relevance, since AD patients are often colonized with *S.aureus*, even in NL skin [4, 84]. Similar but weaker correlations were seen with IgE, while minimal correlations where found with age (Fig. 3a-b).

A robust genomic AD classifier

Because clinical trials with specific and broad therapeutics are being tested in AD [5, 85], establishing a reliable gene set to discriminate between diseased and normal-appearing skin in AD is crucial. Here, we applied the classification algorithm Meta Threshold Gradient Directed Regularization (MTGDR) [41, 42], to determine the smallest set of genes that distinguishes LS from NL AD skin (see Methods). The final model identifies 19 genes (Fig. 3c and Table 2), including both epidermal and dermal genes, emphasizing the importance of both compartments to the disease model.

To assess the translational validity of these 19 discriminating genes, we investigated the effect of various therapies on gene expression using previously published studies with Dupilumab (300 mg, 4 weeks of treatment) [10], Cyclosporin A (CsA; at 2 and 12 weeks) [12], and narrow band UVB/NB-UVB (12 weeks of treatment) [11], shown in Table 2. Reversal of disease phenotype to the NL state was observed in 18 of the 19 discriminating genes. Overall, a higher reversal was seen with CsA, a broad immune suppressant [86, 87], particularly after 12 weeks of treatment, with an average recovery of 94.64 % (see Table 2).

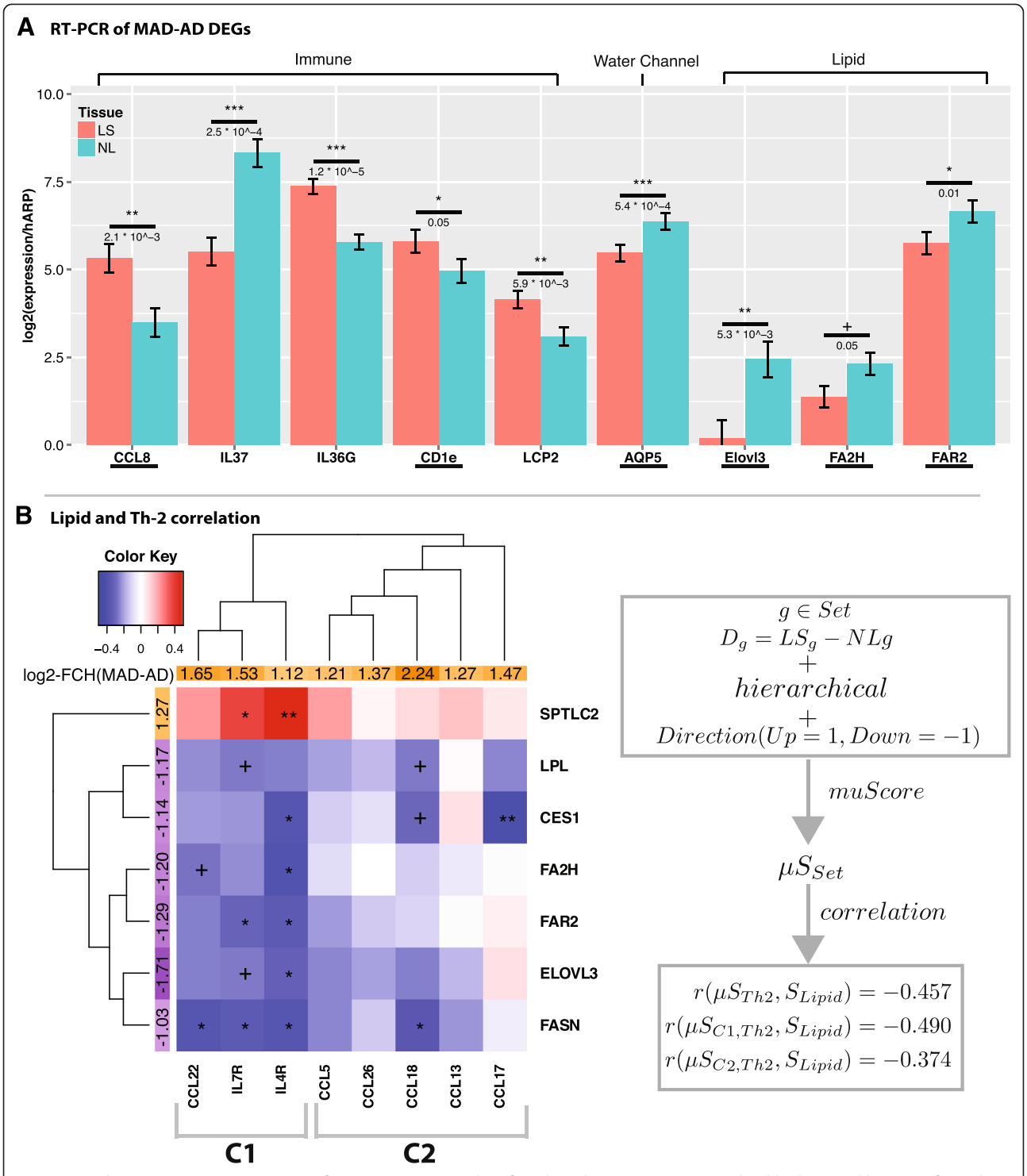

Fig. 2 a Barplot representing means ± SEM of RT-PCR expression values for selected MADAD DEGs, normalized by *hARP* and log2 transformed. Underlined genes represent those not detected in any of the included datasets (IDD-genes). **b** Multivariate correlation between lipid and Th2-related genes dysregulations. Stars indicate the corresponding significance levels (+ ≤0.1, * ≤ 0.05, ** ≤0.01), while the correlations are shown from negative (−0.05, dark blue) to positive (0.05, dark red). The correlation data structure was assessed with Euclidean distance and complete agglomeration hierarchical clustering. Note that the right section gives a schematic overview of the gene set analysis and the corresponding correlation coefficients for the overall Th2 vs Lipid comparison and the sub-comparisons of C1 vs Lipid and C2 vs Lipid (see Additional file 15: Table E10 for corresponding BH adjusted p-values)

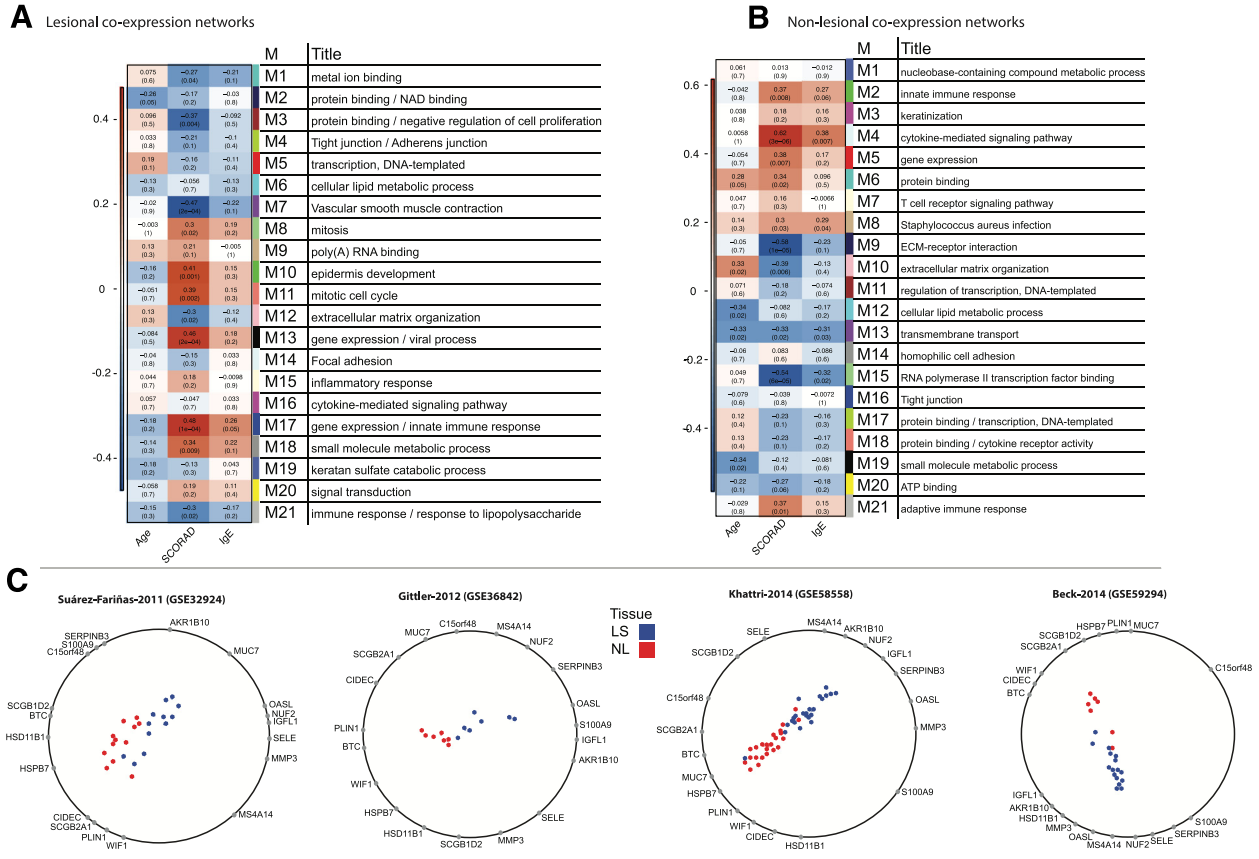

Fig. 3 Module eigen-genes from weighted gene co-expression network analysis (WGCNA), correlated with Age, SCORAD and IgE, including annotation of top overrepresented BP GO-terms, KEGG Pathways or curated inflammatory skin diseases related gene-sets in (**a**) Lesional and (**b**) Non-lesional co-expression networks. Numbers in each cell represent the correlations with the respective trait and the associated p-values (see Additional file 16: Tables E11 and Additional file 17: Table E12 for corresponding BH adjusted p-values). **c** Radviz plots showing the separation of the lesional (LS) and non-lesional (NL) samples, as defined by the 19 genes signature identified by the MTGDR classifier (see Additional file 18: Table E13 for raw MTGDR results)

Among the genes down-regulated with treatment are inflammatory genes (S100A9, SELE) previously associated with AD [9, 59, 88]. Genes up-regulated with treatment (particularly with long-term CsA) include perilipin [89] and hydroxysteroid dehydrogenase [90], which are involved in lipid and steroid metabolism, respectively.

The LS and NL dysregulation in the MADAD correlates with the treatment change induced by CsA ($r = 0.99$; $p = 2.5*10^{-14}$), dupilumab ($r = 0.45$; $p = 0.189$), and UBV ($r = 0.90, p = 0.001$) treatments, leading to restoration of gene expression similar to that seen in NL skin (Additional file 14: Figure E4).

Discussion

A meta-analytic approach utilizes statistical processing and analysis to merge microarray studies from various populations and investigators, resulting in a single value that represents the estimated differential expression level of a gene between LS and NL skin. Combining multiple studies in a meta-analysis produces findings that more precisely reflect the differential expression of genes in a population, representing an accurate molecular characterization of a disease with increased power compared to individual analyses.

To address potential issues regarding meta-analysis application in gene expression studies, including laboratory effects, variations between probes and differential platforms, we planned this analysis beginning with data selection, through pre-processing and filtering, and finally to the meta-analysis model. This pipeline included the adjustment for study-related batch effects to minimize superficial inter-study discordance caused mainly by random noise and technical differences. Although in general this adjustment risk may confound true biological differences, we found no differences in disease severity, IgE and age across the four cohorts and thus feel confident that true biological differences are unlikely to be confounded. The resulting list of DEGs is presented here as a Meta-Analysis Derived Atopic Dermatitis (MADAD) transcriptome, utilizing 4 separate microarray studies for

Table 2 MTGDR robust classifier genes, compared to treatment response, and indication of compartmental allocation as defined by Esaki et al. [63]

SYMBOL	LAYER	logFCH (MAD-AD)	logFCH (Dupilumab, 300 mg, W4)	logFCH (Cyclosporin, W2)	logFCH (Cyclosporin, W12)	logFCH (UVB, W12)	Genename	Recovery (Dupilumab, 300 mg, W4)	Recovery (Cyclosporin, W2)	Recovery (Cyclosporin, W12)	Recovery (UVB, W12)
IGFL1	E	3.5	−2.4[a]	−2.6[a]	−3.6[a]	−2.3[a]	IGF-like family member 1	68.60	74.81	101.60	64.33
OASL	D	2.9	−2.7[a]	−2.7[a]	−3.3[a]	−1.8[a]	2'-5'-oligoadenylate synthetase-like	93.07	93.24	112.20	60.33
SELE	D	2.4	−2.9[a]	−1.6[a]	−1.6[a]	−2.3[a]	selectin E	121.06	66.99	66.24	94.94
AKR1B10	E	3.2	−1.3	−3.2[a]	−4.0[a]	−3.0[a]	aldo-keto reductase family 1, member B10 (aldose reductase)	42.39	100.29	127.48	95.22
MS4A14	D	1.4	−2.0[a]	−1.2[a]	−1.4[a]	0.0	membrane-spanning 4-domains, subfamily A, member 14	149.43	84.71	102.42	0.00
NUF2	E	1.4	−2.2[a]	−1.4[a]	−1.4[a]	−0.9	NUF2, NDC80 kinetochore complex component	155.33	96.79	96.65	59.46
S100A9	E	3.8	−1.1	−3.7[a]	−4.5[a]	−2.2[a]	S100 calcium binding protein A9	27.95	96.75	116.47	57.26
SERPINB3	E	3.8	−1.9	−3.2[a]	−3.8[a]	−2.4[a]	serpin peptidase inhibitor, clade B (ovalbumin), member 3	50.29	85.47	101.40	62.98
C15orf48	E	1.0	−0.9	−1.0	−1.3[a]	−2.1[a]	chromosome 15 open reading frame 48	93.70	103.85	131.53	211.69
MMP3	D	1.1	−4.0[a]	−2.0[a]	−0.9	−0.3	matrix metallopeptidase 3 (stromelysin 1, progelatinase)	374.65	181.39	81.06	25.91
MUC7		−1.2	−0.1	0.0	0.0	1.1	mucin 7, secreted	−9.82	0.00	0.00	87.60
HSPB7	D	−1.6	1.6	0.6	1.7[a]	0.2	heat shock 27 kDa protein family, member 7 (cardiovascular)	102.98	37.95	107.88	13.51
SCGB1D2	D	−1.2	0.3	0.5	1.2[a]	0.0	secretoglobin, family 1D, member 2	25.96	43.28	100.97	0.00
BTC	E	−2.1	−0.1	1.0	1.3[a]	1.3[a]	betacellulin	−6.53	48.15	65.56	65.17
CIDEC		−1.7	2.1	1.2[a]	1.8[a]	0.0	cell death-inducing DFFA-like effector c	126.22	72.11	106.23	−2.38
HSD11B1	E	−2.3	−1.8	0.1	2.1[a]	1.0[a]	hydroxysteroid (11-beta) dehydrogenase 1	−77.60	5.69	91.93	44.65
PLIN1		−1.9	1.9	1.7[a]	2.0[a]	0.3	perilipin 1	98.89	85.20	103.82	12.83
SCGB2A1	D	−1.8	−0.1	0.9	1.7[a]	1.5[a]	secretoglobin, family 2A, member 1	−7.33	50.36	92.70	80.79
WIF1	D	−2.2	0.7	1.2	2.1[a]	1.3[a]	WNT inhibitory factor 1	29.58	52.56	92.11	58.40
E = Epidermis, D = Dermis (Esaki et al. [63])							Average	76.78	72.61	94.64	57.51

[a]Indicate FDR ≤ 0.05

a total of 97 samples. It is our hope that the MADAD will prove helpful to investigators who may benefit from our robust characterization of the AD phenotype.

Similar to the MAD psoriasis transcriptome, our meta-analysis approach resulted in a more concise number of DEGs than that found in the individual studies [25]. However, this set of DEGs provides a more biologically relevant and powerful AD phenotype compared with previous studies [12], since important inflammatory and barrier pathways are more significantly enriched compared to individual studies, as is often observed with meta-analysis derived transcriptomes [91].

Our transcriptome is the first association of AD genomic fingerprinting with the atherosclerosis signaling pathway, which includes genes associated with vascular inflammation (SELE, IL-37, S100A8) [63, 77]. SELE has been independently associated with coronary heart disease and carotid artery atherosclerosis, and its expression in the vascular endothelium of the dermis of AD patients has also been observed [51, 88]. This supports the emerging view of AD as a systemic disease, which, like psoriasis, extends far beyond the skin [92, 93].

We have recently shown increased systemic immune activation in blood of moderate-to-severe AD patients among both skin homing and systemic T-cell subsets [94]. Furthermore, when comparing blood moderate-to-severe psoriasis and AD patients, we have shown that AD is associated with systemic activation and increased polar differentiation of effector and memory T-cell subsets, with higher and persistent activation within skin homing subsets. (Czarnowicki et al.-In press) AD patients also demonstrated higher levels of ICOS activation in circulating skin-homing subsets, (Czarnowicki- In press) consistent with the significant overrepresentation of ICOS signaling in our IPA analysis.

In large cohort studies, AD has also been recently associated with a variety of systemic diseases including inflammatory bowel disease [95, 96], Type 1 Diabetes Mellitus [97], and ADHD [98], providing further evidence for its systemic nature. Additionally, AD, like psoriasis, was recently shown to be associated with increased vascular inflammation using CT imaging [99–101]. The association of AD with systemic involvement emphasizes the great unmet need among severe AD patients for systemic therapeutic approaches, which are now in clinical trials (NCT00638989) [10, 18].

An interesting association between barrier defects and vascular inflammation in AD may be represented by the gene SPTLC2, which encodes a SPT, the rate-limiting enzyme in de novo synthesis of sphingomyelin and ceramides, and which has also been shown to influence atherosclerosis. Plasma sphingomyelin level was found to be an independent risk factor for coronary artery disease and is associated with subclinical atherosclerosis in humans [102, 103]. In ApoE knockout mice, inhibition of SPT resulted in improved lipid profiles and prevented the development of atherosclerotic lesions [104]. Sphingomyelin is proposed to affect atherosclerosis by influencing lipid metabolism and regulating cell proliferation and apoptosis to modulate plaque growth and stability [105]. SPTLC2 increases with epidermal barrier abnormalities [75], as was observed in our MADAD transcriptome, and may be related to the previously unacknowledged systemic vascular inflammation in AD.

Lipid and differentiation abnormalities represent the hallmark of defective barrier function in AD [106, 107]. The Th2 cytokine effects on inhibition of terminal differentiation genes (e.g. filaggrin, loricrin) have been well documented by in vitro [1, 78] and in vivo studies [15, 108]. While the effects of Th2 cytokines on suppression of epidermal lipids have become recently available in model systems [78], our paper is the first to show negative correlations between expression of Th2 cytokines and epidermal lipids. It is established that AD LS skin shows alterations in lipid composition of the stratum corneum [109], with decreases in long-chain ceramides and free fatty acids in addition to disorganized lipid structure [107]. While Th1 cytokines, including TNFα and IFNγ, have been shown to induce ceramide synthesis, Th2 cytokines (including IL-4) inhibit the production of ceramides necessary for proper barrier function [76, 110]. Our findings support these in vitro models, and show significant negative correlations between increased Th2 cytokine production and decreased lipid expression.

We also identified for the first time as differentially expressed in AD several genes involved in lipid metabolism. These include FA2H, encoding protein essential to the de novo synthesis of specific ceramides that are critical in maintaining the permeability barrier of the epidermis [111, 112], and ELOVL3, encoding a protein involved in the elongation of long chain fatty acids and essential in prevention of transepidermal water loss [113, 114]. While not involved in fatty acid synthesis, aquaporin 5/AQP5 is a water channel that was found to be decreased in LS AD skin [115–117].

The network analysis of MADAD DEGs shows a significant correlation between AD disease activity/SCORAD and the *S. aureus* module in NL skin, emphasizing the role of colonization and infection in the onset of immune activation in background skin. *S. aureus* colonization/infection has been shown to occur at significantly higher rates in both LS and NL AD skin compared to healthy controls [118–120], and was shown to induce Th2 and Th22 immune activation [84, 121–123]. In LS skin, viral and innate immune process modules were significantly positively correlated with SCORAD, emphasizing the association between reactions to external pathogens and active inflammation in AD [121].

The treatment effect on the 19 discriminatory genes highlights the diverse mechanistic effects of these therapies with several observations worth mentioning. First, MMP3, a marker of general inflammation, displays an impressive recovery with the targeted therapy dupilumab compared to the more nonspecific immune suppressant treatments. This inflammatory gene improved over 300 % in only 4 weeks of treatment with dupilumab, while long-term treatment with CsA and UVB did not reach 100 % recovery. This may suggest the ability of dupilumab to suppress immune dysregulation in AD in a shorter time-frame than with less specific agents. Another noteworthy gene is Selectin E, encoding a protein involved in leukocyte extravasation, which also showed higher levels of recovery in dupilumab compared to CsA and UVB therapy. The difference in these markers may be related to the mechanism of action of each drug; UVB has direct effects on keratinocytes and thus mainly mediates signals originating there, while CsA is a nonspecific inhibitor of T-cells, B-cells and related pathways. Dupilumab more specifically modulates IL-4/IL-13 signaling, which has been implicated in the pathogenesis of AD, and this may account for the impressive recovery seen in genes central to the inflammatory response generated by AD.

Conclusions

This meta-analysis provides a stable and robust AD transcriptome worthy of future biomarker selection and evaluation of treatment response. The value of a standardized AD transcriptome will only increase with the bench-to-bedside translational approach, as a standardized measure of treatment response that cannot be confounded with placebo effects. This meta-analysis provides an integrative model of AD, emphasizing both immune and barrier abnormalities and also highlighting the systemic nature of the disease.

Additional files

Additional file 1: Supplementary materials and methods. (DOCX 111 kb)

Additional file 2: Table E9. Primer IDs for RT-PCR analysis. (XLSX 37 kb)

Additional file 3: Figure E1. A) Prisma. B) MADAD Datasets. C) Meta-Analysis Workflow. (PDF 608 kb)

Additional file 4: Table E1. All datasets intially considered before applying inclusion/exclusion criteria. (DOCX 65 kb)

Additional file 5: Table E2. Consensus of re-analyized included datasets (by Probes). (XLSX 60 kb)

Additional file 6: Figure E2. QQ plot. Comparison of parameters. (PDF 1005 kb)

Additional file 7: Table E3. ALL MADAD DEGs (FCH ≥ 2, FDR ≤ 0.05). (XLSX 171 kb)

Additional file 8: Table E4. MADAD – Ingenuity Pathway Analysis. (XLSX 33 kb)

Additional file 9: Table E5. Khattri 2014 (GSE58558) – Ingenuity Pathway Analysis. (XLSX 26 kb)

Additional file 10: Figure E3. A) Inflammatory Skin Disease Gene Sets. B) MADAD IDD-DEGs IPA Canonical Pathways. (PDF 85 kb)

Additional file 11: Table E6. IPA Pathways and GO terms IDD genes. (XLSX 9 kb)

Additional file 12: Table E7. Overrepresented Hub30 Genes and module names. (LS) (XLSX 38 kb)

Additional file 13: Table E8. Overrepresented Hub30 Genes and module names. (NL) (XLSX 47 kb)

Additional file 14: Figure E4. logFCHs correlations of MADAD and treatments A) Dupilumab (300mg), B) Cyclosporin (W12), and C) UVB. (PDF 42 kb)

Additional file 15: Table E10. Adjusted P-values for the significance indicators in Figure 2B. (XLSX 8 kb)

Additional file 16: Table E11. BH adjusted p-values WGCNA LS Modules. (XLSX 9 kb)

Additional file 17: Table E12. BH adjusted p-values WGCNA NL Modules. (XLSX 9 kb)

Additional file 18: Table E13. MTGDR results. (XLSX 9 kb)

Abbreviations

AD: Atopic dermatitis; CsA: Cyclosporin A; DEGs: Differentially expressed genes (logFCH ≥ 1 and fdr ≤ 0.05); FDR: False Discovery Rate; FEM: Fixed-effects model (special case of REM); ICC: Integrated Correlation Coefficient; IDD: Integration-driven discovery; IgE: Immunoglobulin E; IPA: Ingenuity pathway analysis; LS: Lesional; MAD-AD: Meta-analysis derived AD; MTGDR: Meta Threshold Gradient Directed Regularization; NL: Non-lesional; PRISMA: Preferred Reporting Items for Systematic Reviews and Meta-Analyses; REM: Random-effects model; RT-PCR: Quantitative Reverse Transcription PCR; RPLP0: Ribosomal protein, large, P0 (formerly termed *human acidic ribosomal protein P0*/hARP); S. aureus: Staphylococcus aureus; SCORAD: Scoring of Atopic Dermatitis; SPT: Serine palmitoyltransferase; WGCNA: Weighted gene co-expression network analysis.

Competing interests

DAE is partly funded by the Danish Ministry of Science and Higher Education and LEO Pharma AS. TL is employed by LEO Pharma AS. All other authors have no competing interests to disclose.

Authors' contributions

DAE carried out the main statistical and bioinformatics analysis, and prepared the manuscript. DM prepared the manuscript and carried out biological assessment and evaluations of the statistical results. JGK participated in the design of the study and manuscript preparation. CTW advised and participated in the bioinformatics analysis. TW and ST carried out the classification analysis. TL participated in the design of the study and manuscript preparation. EGY participated in the design of the study and directed manuscript preparation. MSF designed the study, directed manuscript preparation, and directed the statistical analysis. All authors have read and approved the final manuscript.

Authors' information

Not applicable.

Availability of data and materials

Not applicable.

Acknowledgements

The authors thank Joel Correa da Rosa, Sandra Garcet, and Troels Marstrand for helpful discussions on the analysis pipeline. This work was supported by LEO Pharma AS and the Danish Ministry of Science and Higher Education.

Funding

This work was supported by the danish ministry of scienceand higher education in terms of partly funding of a PhD fellowship (http://ufm.dk/en/the-minister-and-theministry/organisation/the-ministry).

Author details

[1]The Laboratory for Investigative Dermatology, The Rockefeller University, New York, NY, USA. [2]Department of Dermatology, Icahn School of Medicine

at Mount Sinai, New York, NY, USA. [3]Molecular Biomedicine, LEO Pharma AS, Ballerup, Denmark. [4]Center for Biological Sequence Analysis, Department of Systems Biology, Technical University of Denmark, Kgs. Lyngby, Denmark. [5]Columbia University, College of Physicians and Surgeons, New York, NY, USA. [6]School of Life Science, Jilin University, 2699 Qianjin Street, Changchun, Jilin 130012, China. [7]Department of Population Health Science and Policy, Icahn School of Medicine at Mount Sinai, New York, NY, USA. [8]Icahn Institute for Genomics and Multiscale Biology at Mount Sinai, Icahn School of Medicine at Mount Sinai, New York, NY, USA.

Received: 23 March 2015 Accepted: 11 September 2015
Published online: 12 October 2015

References

1. Boguniewicz M, Leung DYM. Atopic dermatitis: a disease of altered skin barrier and immune dysregulation. Immunol Rev. 2011;242(1):233–46.
2. Leung DYM. New insights into atopic dermatitis: role of skin barrier and immune dysregulation. Allergol Int. 2013;62(2):151–61.
3. Dhingra N, Suarez-Farinas M, Fuentes-Duculan J, Gittler JK, Shemer A, Raz A, et al. Attenuated neutrophil axis in atopic dermatitis compared to psoriasis reflects TH17 pathway differences between these diseases. J Allergy Clin Immunol. 2013;132(2):498–501.e3.
4. Malajian D, & Guttman-Yassky E. New pathogenic and therapeutic paradigms in atopic dermatitis. Cytokine. 2015;73(2):311-318.
5. N & Guttman-Yassky E. The translational revolution and use of biologics in patients with inflammatory skin diseases. Journal of Allergy and Clinical Immunology. 2015;135(2):324-336.
6. Olsson M, Broberg A, Jernås M, Carlsson L, Rudemo M, Suurküla M, et al. Increased expression of aquaporin 3 in atopic eczema. Allergy. 2006;61(9):1132–7.
7. Guttman-Yassky E, Suárez-Fariñas M, Chiricozzi A, Nograles KE, Shemer A, Fuentes-Duculan J, et al. Broad defects in epidermal cornification in atopic dermatitis identified through genomic analysis. J Allergy Clin Immunol. 2009;124(6):1235–1244.e58.
8. Elias PM, Hatano Y, Williams ML. Basis for the barrier abnormality in atopic dermatitis: Outside-inside-outside pathogenic mechanisms. J Allergy Clin Immunol. 2008;121(6):1337–43.
9. Gittler JK, Shemer A, Suárez-Fariñas M, Fuentes-Duculan J, Gulewicz KJ, Wang CQF, et al. Progressive activation of T(H)2/T(H)22 cytokines and selective epidermal proteins characterizes acute and chronic atopic dermatitis. J Allergy Clin Immunol. 2012;130(6):1344–54.
10. Beck L, Thaçi D, Hamilton JD, Graham NM, Bieber T, Rocklin R, et al. Dupilumab Treatment in Adults with Moderate-to-Severe Atopic Dermatitis. N Engl J Med. 2014;371(2):130–9.
11. Tintle S, Shemer A, Suárez-Fariñas M, Fujita H, Gilleaudeau P, Sullivan-Whalen M, et al. Reversal of atopic dermatitis with narrow-band UVB phototherapy and biomarkers for therapeutic response. J Allergy Clin Immunol. 2011;128(3):583–93.e1–4.
12. Khattri S, Shemer A, Rozenblit M, Dhingra N, Czarnowicki T, Finney R, & Guttman-Yassky E. Cyclosporine in patients with atopic dermatitis modulates activated inflammatory pathways and reverses epidermal pathology. Journal of Allergy and Clinical Immunology. 2014;133(6):1626-634.
13. Jensen JM, Pfeiffer S, Witt M, Bräutigam M, Neumann C, Weichenthal M, et al. Different effects of pimecrolimus and betamethasone on the skin barrier in patients with atopic dermatitis. J Allergy Clin Immunol. 2009;123:1124–33.
14. Plager A, Leontovich AA, Henke SA, Davis MDP, McEvoy MT, Sciallis GF, et al. Early cutaneous gene transcription changes in adult atopic dermatitis and potential clinical implications. Exp Dermatol. 2007;16(1):28–36.
15. Suárez-Fariñas M, Tintle SJ, Shemer A, Chiricozzi A, Nograles K, Cardinale I, et al. Nonlesional atopic dermatitis skin is characterized by broad terminal differentiation defects and variable immune abnormalities. J Allergy Clin Immunol. 2011;127(4):954–64.e1–4.
16. Zaba LC, Suárez-Fariñas M, Fuentes-Duculan J, Nograles KE, Guttman-Yassky E, Cardinale I, et al. Effective treatment of psoriasis with etanercept is linked to suppression of IL-17 signaling, not immediate response TNF genes. J Allergy Clin Immunol. 2009;124(5):1022–10.e1–395.
17. Krueger JG, Fretzin S, Suárez-Fariñas M, Haslett PA, Phipps KM, Cameron GS, et al. IL-17A is essential for cell activation and inflammatory gene circuits in subjects with psoriasis. J Allergy Clin Immunol. 2012;130(1):1–18.
18. Hamilton JD, Suárez-Fariñas M, Dhingra N, Cardinale I, Li X, Kostic A, et al. Dupilumab improves the molecular signature in skin of patients with moderate-to-severe atopic dermatitis. J Allergy Clin Immunol. 2014;134(6):1293–300.
19. Jiang K, Frank MB, Chen Y, Osban J, Jarvis JN. Genomic characterization of remission in juvenile idiopathic arthritis. Arthritis Res Ther. 2013;15(4):R100.
20. Cahan P, Rovegno F, Mooney D, Newman JC, St Laurent G, McCaffrey TA. Meta-analysis of microarray results: challenges, opportunities, and recommendations for standardization. Gene. 2007;401(1–2):12–8.
21. Ramasamy A, Mondry A, Holmes CC, Altman DG. Key issues in conducting a meta-analysis of gene expression microarray datasets. PLoS Med. 2008;5(9):e184.
22. Zakharkin SO, Kim K, Mehta T, Chen L, Barnes S, Scheirer KE, et al. Sources of variation in Affymetrix microarray experiments. BMC Bioinformatics. 2005;6:214.
23. Suárez-Fariñas M, Noggle S, Heke M, Hemmati-Brivanlou A, Magnasco MO. Comparing independent microarray studies: the case of human embryonic stem cells. BMC Genomics. 2005;6:99.
24. Suárez-Fariñas M, Lowes MA, Zaba LC, Krueger JG. Evaluation of the psoriasis transcriptome across different studies by gene set enrichment analysis (GSEA). PLoS One. 2010;5(4):e10247.
25. Tian S, Krueger JG, Li K, Jabbari A, Brodmerkel C, Lowes MA, et al. Meta-analysis derived (MAD) transcriptome of psoriasis defines the 'core' pathogenesis of disease. PLoS One. 2012;7(9):e44274.
26. Chang L-C, Lin H-M, Sibille E, Tseng GC. Meta-analysis methods for combining multiple expression profiles: comparisons, statistical characterization and an application guideline. BMC Bioinformatics. 2013;14(vi):368.
27. Choi JK, Yu U, Kim S, Yoo OJ. Combining multiple microarray studies and modeling interstudy variation. Bioinformatics. 2003;19 Suppl 1:i84–90.
28. Tseng GC, Ghosh D, Feingold E. Comprehensive literature review and statistical considerations for microarray meta-analysis. Nucleic Acids Res. 2012;40(9):3785–99.
29. Liberati A, Altman DG, Tetzlaff J, Mulrow C, Gøtzsche PC, Ioannidis JPA, et al. The PRISMA statement for reporting systematic reviews and meta-analyses of studies that evaluate health care interventions: explanation and elaboration. PLoS Med. 2009;6(7):e1000100.
30. Team R, Core. "R: A language and environment for statistical computing. R Foundation for Statistical Computing, Vienna, Austria, 2012." (2014).
31. Gentleman RC, Carey VJ, Bates DM, Bolstad B, Dettling M, Dudoit S, et al. Bioconductor: open software development for computational biology and bioinformatics. Genome Biol. 2004;5(10):R80.
32. Wu Z, Irizarry RA, Gentleman R, Martinez-Murillo F, Spencer F. A Model-Based Background Adjustment for Oligonucleotide Expression Arrays. J Am Stat Assoc. 2004;99(468):909–17.
33. Johnson WE, Li C, Rabinovic A. Adjusting batch effects in microarray expression data using empirical Bayes methods. Biostatistics. 2007;8(1):118–27.
34. Leek JT, Johnson WE, Parker HS, Jaffe AE, Storey JD. The sva package for removing batch effects and other unwanted variation in high-throughput experiments. Bioinformatics. 2012;28(6):882–3.
35. Leek JT, Scharpf RB, Bravo HC, Simcha D, Langmead B, Johnson WE, et al. Tackling the widespread and critical impact of batch effects in high-throughput data. Nat Rev Genet. 2010;11:733–9.
36. Parmigiani G. A Cross-Study Comparison of Gene Expression Studies for the Molecular Classification of Lung Cancer. Clin Cancer Res. 2004;10(9):2922–7.
37. Benjamini Y, Hochberg Y. Controlling the false discovery rate: a practical and powerful approach to multiple testing. J R Stat Soc. 1995;57(1):289–300.
38. Huang DW, Sherman BT, Lempicki RA. Systematic and integrative analysis of large gene lists using DAVID bioinformatics resources. Nat Protoc. 2009;4:44–57.
39. Suárez-Fariñas M, Arbeit R, Jiang W, Ortenzio FS, Sullivan T, Krueger JG. Suppression of molecular inflammatory pathways by Toll-like receptor 7, 8, and 9 antagonists in a model of IL-23-induced skin inflammation. PLoS One. 2013;8(12):e84634.
40. Langfelder P, Horvath S. WGCNA: an R package for weighted correlation network analysis. BMC Bioinformatics. 2008;9:559.
41. Ma S, Huang J. Regularized gene selection in cancer microarray meta-analysis. BMC Bioinformatics. 2009;10:1.
42. Tian S, Suarez-Farinas M. Multi-TGDR: a regularization method for multi-class classification in microarray experiments. PLoS One. 2013;8(11):e78302.
43. Mitsui H, Suárez-Fariñas M, Belkin DA, Levenkova N, Fuentes-Duculan J, Coats I, et al. Combined use of laser capture microdissection and cDNA microarray analysis identifies locally expressed disease-related genes in focal regions of psoriasis vulgaris skin lesions. J Invest Dermatol. 2012;132(6):1615–26.

44. Rappaport N, Nativ N, Stelzer G, Twik M, Guan-Golan Y, Stein TI, et al. MalaCards: an integrated compendium for diseases and their annotation. Database (Oxford). 2013;2013:bat018.
45. Appace. Solr. 2014.
46. Wittkowski KM, Song T. Nonparametric methods for molecular biology. Methods Mol Biol. 2010;620:105–53.
47. Irizarry RA, Warren D, Spencer F, Kim IF, Biswal S, Frank BC, et al. Multiple-laboratory comparison of microarray platforms. Nat Methods. 2005;2(5):345–50.
48. Lowes MA, Suárez-Fariñas M, Krueger JG. Immunology of psoriasis. Annu Rev Immunol. 2014;32:227–55.
49. Panzer R, Blobel C, Fölster-Holst R, Proksch E. TLR2 and TLR4 expression in atopic dermatitis, contact dermatitis and psoriasis. Exp Dermatol. 2014;23(5):364–6.
50. Kuo I-H, Carpenter-Mendini A, Yoshida T, McGirt LY, Ivanov AI, Barnes KC, et al. Activation of epidermal toll-like receptor 2 enhances tight junction function: implications for atopic dermatitis and skin barrier repair. J Invest Dermatol. 2013;133(4):988–98.
51. Hwang SJ, Ballantyne CM, Sharrett AR, Smith LC, Davis CE, Gotto AM, et al. Circulating adhesion molecules VCAM-1, ICAM-1, and E-selectin in carotid atherosclerosis and incident coronary heart disease cases: the Atherosclerosis Risk In Communities (ARIC) study. Circulation. 1997;96(12):4219–25.
52. Kiechl S, Paré G, Barbalic M, Qi L, Dupuis J, Dehghan A, et al. Association of variation at the ABO locus with circulating levels of soluble intercellular adhesion molecule-1, soluble P-selectin, and soluble E-selectin: a meta-analysis. Circ Cardiovasc Genet. 2011;4(6):681–6.
53. Mead JR, Ramji DP. The pivotal role of lipoprotein lipase in atherosclerosis. Cardiovasc Res. 2002;55(2):261–9.
54. Chen Q, Razzaghi H, Demirci FY, Kamboh MI. Functional significance of lipoprotein lipase HindIII polymorphism associated with the risk of coronary artery disease. Atherosclerosis. 2008;200(1):102–8.
55. Goldberg IJ. Lipoprotein lipase and lipolysis: central roles in lipoprotein metabolism and atherogenesis. J Lipid Res. 1996;37(4):693–707.
56. Xu X, Wang L, Xu C, Zhang P, Yong F, Liu H, et al. Variations in matrix metalloproteinase-1, −3, and −9 genes and the risk of acute coronary syndrome and coronary artery disease in the Chinese Han population. Coron Artery Dis. 2013;24(4):259–65.
57. Abilleira S, Bevan S, Markus HS. The role of genetic variants of matrix metalloproteinases in coronary and carotid atherosclerosis. J Med Genet. 2006;43(12):897–901.
58. Averill MM, Kerkhoff C, Bornfeldt KE. S100A8 and S100A9 in cardiovascular biology and disease. Arterioscler Thromb Vasc Biol. 2012;32(2):223–9.
59. Jin S, Park CO, Shin JU, Noh JY, Lee YS, Lee NR, et al. DAMP molecules S100A9 and S100A8 activated by IL-17A and house-dust mites are increased in atopic dermatitis. Exp Dermatol. 2014;23(12):938–41.
60. Ji Q, Zeng Q, Huang Y, Shi Y, Lin Y, Lu Z, et al. Elevated plasma IL-37, IL-18, and IL-18BP concentrations in patients with acute coronary syndrome. Mediators Inflamm. 2014;2014:165742.
61. Inouye M, Ripatti S, Kettunen J, Lyytikäinen L-P, Oksala N, Laurila P-P, et al. Novel Loci for metabolic networks and multi-tissue expression studies reveal genes for atherosclerosis. PLoS Genet. 2012;8(8):e1002907.
62. Tregouet DA, Barbaux S, Poirier O, Blankenberg S, Bickel C, Escolano S, et al. SELPLG gene polymorphisms in relation to plasma SELPLG levels and coronary artery disease. Ann Hum Genet. 2003;67(Pt 6):504–11.
63. Esaki H, Ewald DA, Ungar B, Rozenblit M. Identification of novel immune and barrier genes in atopic dermatitis by means of laser capture microdissection. J Allergy Clin Immunol. 2015;135(1):153–63.
64. Choi UY, Kang JS, Hwang YS, Kim YJ. Oligoadenylate synthase-like (OASL) proteins: dual functions and associations with diseases. Experimental & molecular medicine. 2015;47(3):e144.
65. Wensink AC, Hack CE, Bovenschen N. Granzymes Regulate Proinflammatory Cytokine Responses. J Immunol. 2015;194(2):491–7.
66. Westerberg R, Mansson JE, Golozoubova V, Shabalina IG, Backlund EC, Tvrdik P, et al. ELOVL3 is an important component for early onset of lipid recruitment in brown adipose tissue. J Biol Chem. 2006;281(8):4958–68.
67. Turlo K, Leung CS, Seo JJ, Goulbourne CN, Adeyo O, Gin P, et al. Equivalent binding of wild-type lipoprotein lipase (LPL) and S447X-LPL to GPIHBP1, the endothelial cell LPL transporter. Biochim Biophys Acta. 2014;1841(7):963–9.
68. Goulbourne CN, Gin P, Tatar A, Nobumori C, Hoenger A, Jiang H, et al. The GPIHBP1-LPL complex is responsible for the margination of triglyceride-rich lipoproteins in capillaries. Cell Metab. 2014;19(5):849–60.
69. Pan Y-S, Lee Y-S, Lee Y-L, Lee W-C, Hsieh S-Y. Differentially profiling the low-expression transcriptomes of human hepatoma using a novel SSH/microarray approach. BMC Genomics. 2006;7:131.
70. Tortola L, Rosenwald E, Abel B, Blumberg H, Schäfer M, Coyle AJ, et al. Psoriasiform dermatitis is driven by IL-36-mediated DC-keratinocyte crosstalk. J Clin Invest. 2012;122(11):3965–76.
71. Nold MF, Nold-Petry CA, Zepp JA, Palmer BE, Bufler P, Dinarello CA. IL-37 is a fundamental inhibitor of innate immunity. Nat Immunol. 2010;11(11):1014–22.
72. da Rosa JC, Malajian D, Shemer A, Rozenblit M, Dhingra N, Czarnowicki T, et al. Patients with atopic dermatitis have attenuated and distinct contact hypersensitivity responses to common allergens in skin. Journal of Allergy and Clinical Immunology, 2015:135(3):712-20.
73. van Smeden J, Janssens M, Kaye ECJ, Caspers PJ, Lavrijsen AP, Vreeken RJ, et al. The importance of free fatty acid chain length for the skin barrier function in atopic eczema patients. Exp Dermatol. 2014;23:45–52.
74. Lee Y, Je Y-J, Lee S-S, Li ZJ, Choi D-K, Kwon Y-B, et al. Changes in transepidermal water loss and skin hydration according to expression of aquaporin-3 in psoriasis. Ann Dermatol. 2012;24(2):168–74.
75. Stachowitz S, Alessandrini F, Abeck D, Ring J, Behrendt H. Permeability barrier disruption increases the level of serine palmitoyltransferase in human epidermis. J Invest Dermatol. 2002;119(5):1048–52.
76. Sawada E, Yoshida N, Sugiura A, Imokawa G. Th1 cytokines accentuate but Th2 cytokines attenuate ceramide production in the stratum corneum of human epidermal equivalents: an implication for the disrupted barrier mechanism in atopic dermatitis. J Dermatol Sci. 2012;68(1):25–35.
77. Tanno O, Ota Y, Kitamura N, Katsube T, Inoue S. Nicotinamide increases biosynthesis of ceramides as well as other stratum corneum lipids to improve the epidermal permeability barrier. Br J Dermatol. 2000;143(3):524–31.
78. Danso MO, van Drongelen V, Mulder A, van Esch J, Scott H, van Smeden J, et al. TNF-α and Th2 Cytokines Induce Atopic Dermatitis-Like Features on Epidermal Differentiation Proteins and Stratum Corneum Lipids in Human Skin Equivalents. J Invest Dermatol. 2014;134(7):1941–50.
79. Hirota T, Saeki H, Tomita K, Tanaka S, Ebe K, Sakashita M, et al. Variants of C-C motif chemokine 22 (CCL22) are associated with susceptibility to atopic dermatitis: case–control studies. PLoS One. 2011;6(11):e26987.
80. Hussein YM, Shalaby SM, Nassar A, Alzahrani SS, Alharbi AS, Nouh M. Association between genes encoding components of the IL-4/IL-4 receptor pathway and dermatitis in children. Gene. 2014;545(2):276–81.
81. Gao P-S, Rafaels NM, Mu D, Hand T, Murray T, Boguniewicz M, et al. Genetic variants in thymic stromal lymphopoietin are associated with atopic dermatitis and eczema herpeticum. J Allergy Clin Immunol. 2010;125(6):1403–1407.e4.
82. Langfelder P, Horvath S. WGCNA package FAQ. 2014 [Online]. Available: http://labs.genetics.ucla.edu/horvath/CoexpressionNetwork/Rpackages/WGCNA/faq.html. [Accessed: 03-Mar-2015].
83. Hon KL, Ching GK, Ng PC, Leung TF. Exploring CCL18, eczema severity and atopy. Pediatr Allergy Immunol. 2011;22(7):704–7.
84. Niebuhr M, Mamerow D, Heratizadeh A, Satzger I, Werfel T. Staphylococcal alpha-toxin induces a higher T cell proliferation and interleukin-31 in atopic dermatitis. Int Arch Allergy Immunol. 2011;156(4):412–5.
85. Guttman-Yassky E, Dhingra N, Leung DYM. New era of biologic therapeutics in atopic dermatitis. Expert Opin Biol Ther. 2013;13(4):549–61.
86. Rozenblit M, Suarez-Farinas M, Shemer A, Khattri S, Gilleaudeau P, Sullivan-Whalen M, et al. Residual genomic profile after cyclosporine treatment may offer insights into atopic dermatitis reoccurrence. J Allergy Clin Immunol. 2014;134(4):955–7.
87. Brandt C, Pavlovic V, Radbruch A, Worm M, Baumgrass R. Low-dose cyclosporine A therapy increases the regulatory T cell population in patients with atopic dermatitis. Allergy. 2009;64(11):1588–96.
88. Marinović Kulišić S, Lipozenčić J, Gregorović G, Gregurek G, Lacković G, Jurić-Lekić G. Expression of e-selectin in the skin of patients with atopic dermatitis: morphometric study. Acta Dermatovenerol Croat. 2010;18(3):141–5.
89. Tsao C-H, Shiau M-Y, Chuang P-H, Chang Y-H, Hwang J. Interleukin-4 regulates lipid metabolism by inhibiting adipogenesis and promoting lipolysis. J Lipid Res. 2014;55(3):385–97.
90. Morgan SA, McCabe EL, Gathercole LL, Hassan-Smith ZK, Larner DP, Bujalska IJ, et al. 11β-HSD1 is the major regulator of the tissue-specific effects of circulating glucocorticoid excess. Proc Natl Acad Sci U S A. 2014;111(24):E2482–91.
91. Pérez-Montarelo D, Hudson NJ, Fernández AI, Ramayo-Caldas Y, Dalrymple BP, Reverter A. Porcine tissue-specific regulatory networks derived from meta-analysis of the transcriptome. PLoS One. 2012;7(9):e46159.

92. Voiculescu VM, Lupu M, Papagheorghe L, Giurcaneanu C, Micu E. Psoriasis and Metabolic Syndrome–scientific evidence and therapeutic implications. Journal of medicine and life. 2014;7(4):468.
93. Oliveira Mde F, Rocha Bde O, Duarte GV. Psoriasis: classical and emerging comorbidities. An Bras Dermatol. 2015;90(1):9–20.
94. Czarnowicki T, Gonzalez J, Shemer A, Malajian D, Xu H, Zheng X, et al. Severe atopic dermatitis is characterized by selective expansion of circulating TH2/TC2 and TH22/TC22, but not TH17/TC17, cells within the skin-homing T-cell population. J Allergy Clin Immunol. 2015.
95. Niwa Y, Sumi H, Akamatsu H. An association between ulcerative colitis and atopic dermatitis, diseases of impaired superficial barriers. J Invest Dermatol. 2004;123(5):999–1000.
96. Myrelid P, Dufmats M, Lilja I, Grinn C, Lannerstad O, Sjödahl R. Atopic manifestations are more common in patients with Crohn disease than in the general population. Scand J Gastroenterol. 2004;39(8):731–6.
97. Cardwell CR, Shields MD, Carson DJ, Patterson CC. A meta-analysis of the association between childhood type 1 diabetes and atopic disease. Diabetes Care. 2003;26(9):2568–74.
98. Schmitt J, Buske-Kirschbaum A, Roessner V. Is atopic disease a risk factor for attention-deficit/hyperactivity disorder? A systematic review. Allergy. 2010;65(12):1506–24.
99. 7 th International Congress of Psoriasis: from Gene to Clinic The Queen Elizabeth II Conference Centre, London, U.K. 11th-13th December 2014. Br. J. Dermatol. 2014;171:6, e105–e173.
100. Dave J, Ahlman MA, Lockshin BN, Bluemke DA, Mehta NN. Vascular inflammation in psoriasis localizes to the arterial wall using a novel imaging technique. J Am Acad Dermatol. 2014;70(6):1137–8.
101. Rose S, Sheth NH, Baker JF, Ogdie A, Raper A, Saboury B, et al. A comparison of vascular inflammation in psoriasis, rheumatoid arthritis, and healthy subjects by FDG-PET/CT: a pilot study. Am J Cardiovasc Dis. 2013;3(4):273–8.
102. Jiang XC, Paultre F, Pearson TA, Reed RG, Francis CK, Lin M, et al. Plasma sphingomyelin level as a risk factor for coronary artery disease. Arterioscler Thromb Vasc Biol. 2000;20(12):2614–8.
103. Nelson JC, Jiang X-C, Tabas I, Tall A, Shea S. Plasma sphingomyelin and subclinical atherosclerosis: findings from the multi-ethnic study of atherosclerosis. Am J Epidemiol. 2006;163(10):903–12.
104. Park T-S, Panek RL, Mueller SB, Hanselman JC, Rosebury WS, Robertson AW, et al. Inhibition of sphingomyelin synthesis reduces atherogenesis in apolipoprotein E-knockout mice. Circulation. 2004;110(22):3465–71.
105. Tabas I. Sphingolipids and atherosclerosis: a mechanistic connection? A therapeutic opportunity? Circulation. 2004;110(22):3400–1.
106. van Smeden J, Janssens M, Gooris GS, Bouwstra JA. The important role of stratum corneum lipids for the cutaneous barrier function. Biochim Biophys Acta. 2014;1841(3):295–313.
107. Janssens M, van Smeden J, Gooris GS, Bras W, Portale G, Caspers PJ, et al. Increase in short-chain ceramides correlates with an altered lipid organization and decreased barrier function in atopic eczema patients. J Lipid Res. 2012;53(12):2755–66.
108. Fujita H, Shemer A, Suárez-Fariñas M, Johnson-Huang LM, Tintle S, Cardinale I, et al. Lesional dendritic cells in patients with chronic atopic dermatitis and psoriasis exhibit parallel ability to activate T-cell subsets. J Allergy Clin Immunol. 2011;128(3):574–82.e1–12.
109. Sääf AM, Tengvall-Linder M, Chang HY, Adler AS, Wahlgren C-FF, Scheynius A, et al. Global expression profiling in atopic eczema reveals reciprocal expression of inflammatory and lipid genes. PLoS One. 2008;3(12):e4017.
110. Hatano Y, Terashi H, Arakawa S, Katagiri K. Interleukin-4 suppresses the enhancement of ceramide synthesis and cutaneous permeability barrier functions induced by tumor necrosis factor-alpha and interferon-gamma in human epidermis. J Invest Dermatol. 2005;124(4):786–92.
111. Hama H. Fatty acid 2-Hydroxylation in mammalian sphingolipid biology. Biochim Biophys Acta. 2010;1801(4):405–14.
112. Pappas A. Epidermal surface lipids. Dermatoendocrinol. 2009;1(2):72–6.
113. Westerberg R, Tvrdik P, Unden AB, Mansson JE, Norlen L, Jakobsson A, et al. Role for ELOVL3 and fatty acid chain length in development of hair and skin function. J Biol Chem. 2004;279(7):5621–9.
114. Fehrenschild D, Galli U, Breiden B, Bloch W, Schettina P, Brodesser S, et al. TCF/Lef1-mediated control of lipid metabolism regulates skin barrier function. J Invest Dermatol. 2012;132(2):337–45.
115. Blaydon DC, Lind LK, Plagnol V, Linton KJ, Smith FJ, Wilson NJ, et al. Mutations in AQP5, encoding a water-channel protein, cause autosomal-dominant diffuse nonepidermolytic palmoplantar keratoderma. Am J Hum Genet. 2013;93(2):330–5.
116. Boury-Jamot M, Daraspe J, Bonte F, Perrier E, Schnebert S, Dumas M, et al. Skin aquaporins: function in hydration, wound healing, and skin epidermis homeostasis. Handb Exp Pharmacol. 2009;190:205–17.
117. Nejsum LN, Kwon TH, Jensen UB, Fumagalli O, Frokiaer J, Krane CM, et al. Functional requirement of aquaporin-5 in plasma membranes of sweat glands. Proc Natl Acad Sci U S A. 2002;99(1):511–6.
118. Breuer K, HAussler S, Kapp A, Werfel T. Staphylococcus aureus: colonizing features and influence of an antibacterial treatment in adults with atopic dermatitis. Br J Dermatol. 2002;147(1):55–61.
119. Higaki S, Morohashi M, Yamagishi T, Hasegawa Y. Comparative study of staphylococci from the skin of atopic dermatitis patients and from healthy subjects. Int J Dermatol. 1999;38(4):265–9.
120. Park H-Y, Kim C-R, Huh I-S, Jung M-Y, Seo E-Y, Park J-H, et al. Staphylococcus aureus Colonization in Acute and Chronic Skin Lesions of Patients with Atopic Dermatitis. Ann Dermatol. 2013;25(4):410–6.
121. Matsui K, Nishikawa A. Peptidoglycan from Staphylococcus aureus induces T(H)2 immune response in mice. J Investig Allergol Clin Immunol. 2012;22(2):80–6.
122. Warner JA, McGirt LY, Beck LA. Biomarkers of Th2 polarity are predictive of staphylococcal colonization in subjects with atopic dermatitis. Br J Dermatol. 2009;160(1):183–5.
123. Niebuhr M, Scharonow H, Gathmann M, Mamerow D, Werfel T. Staphylococcal exotoxins are strong inducers of IL-22: A potential role in atopic dermatitis. J Allergy Clin Immunol. 2010;126(6):1176–83.e4.

Submit your next manuscript to BioMed Central and take full advantage of:

- **Convenient online submission**
- **Thorough peer review**
- **No space constraints or color figure charges**
- **Immediate publication on acceptance**
- **Inclusion in PubMed, CAS, Scopus and Google Scholar**
- **Research which is freely available for redistribution**

Submit your manuscript at
www.biomedcentral.com/submit

BioMed Central

SUPPLEMENTARY MATERIALS AND METHODS

Sample Collection

All samples were collected according to the Preferred Reporting Items for Systematic Reviews and Meta-Analyses (PRISMA) statement.

A total of 28 datasets were detected in Gene Expression Omnibus (GEO) but only datasets evaluating expression data of LS vs. NL skin samples of AD patients were retained for analyses. Datasets run on platforms other than the HGU133Plus 2 chip, subject to treatments, or with non-randomly selected NL or LS samples (e.g. FLG homozygous/heterozygous loss of function mutation), and datasets without NL samples were excluded. When overlapping samples were found between datasets, only one copy was kept.

In total, four microarray datasets were included (GSE32924, GSE36842, GSE58558, GSE59294), including 97 samples (54 LS and 43 NL). “Minimum Information about a Microarray Experiment” (MIAME) was available for all studies.

Pre-processing and Expression Analysis

The pre-processing and statistical analysis of the raw microarray data was carried out using *R* and *Bioconductor* packages.

The raw expression data of the four included datasets were combined, summarized, and normalized using the *GCRMA* algorithm with *quantile-normalization,* taking into account the individual probes’ affinities towards non-specific binding by utilizing probe specific sequence information.

Possible batch effects between the four chosen datasets were accessed by *principal component analysis* (*PCA*) and adjusted for by the empirical bayes method *ComBat* from the *sva* package.

This was followed by a two-level filtering procedure, where the combined datasets were filtered first by the per probe-set *Standard Deviation* (*SD*>0.1) and second by the *Integrated Correlation Coefficient* (*ICC*; mean ICC>0.2) The final analysis was conducted on the remaining 21082 probe sets (out of 54675 total probe sets). The before and after filtering correlations between the datasets was accessed by the average pairwise maximum canonical correlations, calculated by the *MergeMaid* package.

To assess the individual studies effects, model estimation and hypothesis testing for the LS versus NL comparison was performed using the mixed-effect framework of the *limma* package, with patients as a random effect and tissue as a fixed effect. P-values were adjusted for multiple testing using the *Benjamini-Hochberg procedure,* with criteria for differentially expressed genes (DEGs) of absolute fold change (|FCH|) ≥ 2.0 and a false discovery rate (FDR) ≤ 0.05.

Meta-analysis

The formal *random effects model (REM)*, as described by Choi and colleagues in 2003, is given below. Let μ_i be the unbiased effect mean effect size for gene *i* (*i*=1,…,*I*), and Y_{ij} the measured effect size for gene *i* study *j* (*j*=1,…,*J*). Then for gene *i* and dataset/study *j*:

$$Y_{ij} = \theta_{ij} + \varepsilon_{ij} \ , \quad \varepsilon_{ij} \sim N\left(0, s_{ij}^2\right)$$

$$\theta_{ij} = \mu_i + \delta_{ij} \ , \quad \delta_{ij} \sim N(0, \tau_i^2)$$

,where τ_i^2 describes the cross-study variance for gene *i*. An estimate of this variance term is readily found by the DerSimonian and Laird (DL) moments estimator. The error term of the observed effect size is characterized by the within-study variance s_{ij}^2 for a given gene *i* in a given study *j*. Both the measured effect size Y_{ij} and the within-study variance are readily assessable from the initial individual analysis of the included datasets. For gene *i,* the parameter of interest μ_i , the average effect size, and its standard error (*se*) are estimated making use of the DL point estimate for τ_i^2:

$$\hat{\mu}_i(\tau_i^2) = \frac{\sum_{j=1}^{J}(s_{ij}^2 + \tau_i^2)^{-1}\, y_{ij}}{\sum_{j=1}^{J}(s_{ij}^2 + \tau_i^2)^{-1}} \ , \quad se[\hat{\mu}_i(\tau_i^2)] = \sqrt{\frac{1}{\sum_{j=1}^{J}(s_{ij}^2 + \tau_i^2)^{-1}}}$$

The *fixed effect model (FEM)* is a special case of the *REM*, assuming the observed differences in effect sizes to be from sampling error alone, i.e. $\tau_i^2 = 0$. Both a *FEM* and a *REM* were applied in order to effectively estimate the true effect size for each probe. Quantile-quantile plots of Cochran's Q sample quantiles versus the theoretical quantiles of the χ_3^2-distribution (from the general χ_{k-1}^2-distribution, with *k* number of datasets = 4) were applied to assess the most appropriate meta-analysis model (Fig E3).

These estimation and calculation steps were carried out making use of the package *GeneMeta.*

Post-processing

The MAD-AD transcriptome was subject to multiple downstream analyses methods. Integration-driven discovery (IDD) DEGs were defined as those not described in any of the included studies. To explore the functional annotations, overrepresentation analysis was carried out for BP GO-terms and KEGG pathways (both in DAVID), Ingenuity Pathways (*IPA* – www.ingenuity.com , as described), and on previously reported gene-sets.

Furthermore, the normalized LS and NL expression data were subject to Weighted Gene Co-Expression Networks Analysis (WGCNA), in order to detect clusters (modules) of correlated genes and their respective hub genes. The modules of this analysis were subject to trait correlation and corresponding gene-set overrepresentation analysis (see Tables E11-12 for corresponding BH adjusted p-values).

Meta Threshold Gradient Directed Regularization (MTGDR) method proposed by Ma and Huang (2009) was used to select the same set of disease-associated genes while allowing for varied estimates of those genes across different experiments, as we have previously published (see Table E13 for raw MTGDR results).

RT-PCR was analyzed as previously described [43] using the primers and probes listed in Table E9. The expression data from these experiments were analyzed in R applying a *mixed effect model* with tissue as fixed effect and patients as random effect.

Lipid genes were defined as genes related to one of the four groups: *Ceramides*, *Free Fatty Acids*, *Sphingolipids*, and *Cholesteryl Esters*. We searched the genecards database for those terms, and included all genes with a relevance score ≥ 10. Pairwise Pearson correlations were calculated between the gene and patient specific deregulations. Multivariate correlations between sets of genes were calculated making use of the gene set specific μ-scores calculated by the *muStat* package (see Table E10 for BH adjusted Pvalues for Figure 2B).

Figure E1

A)

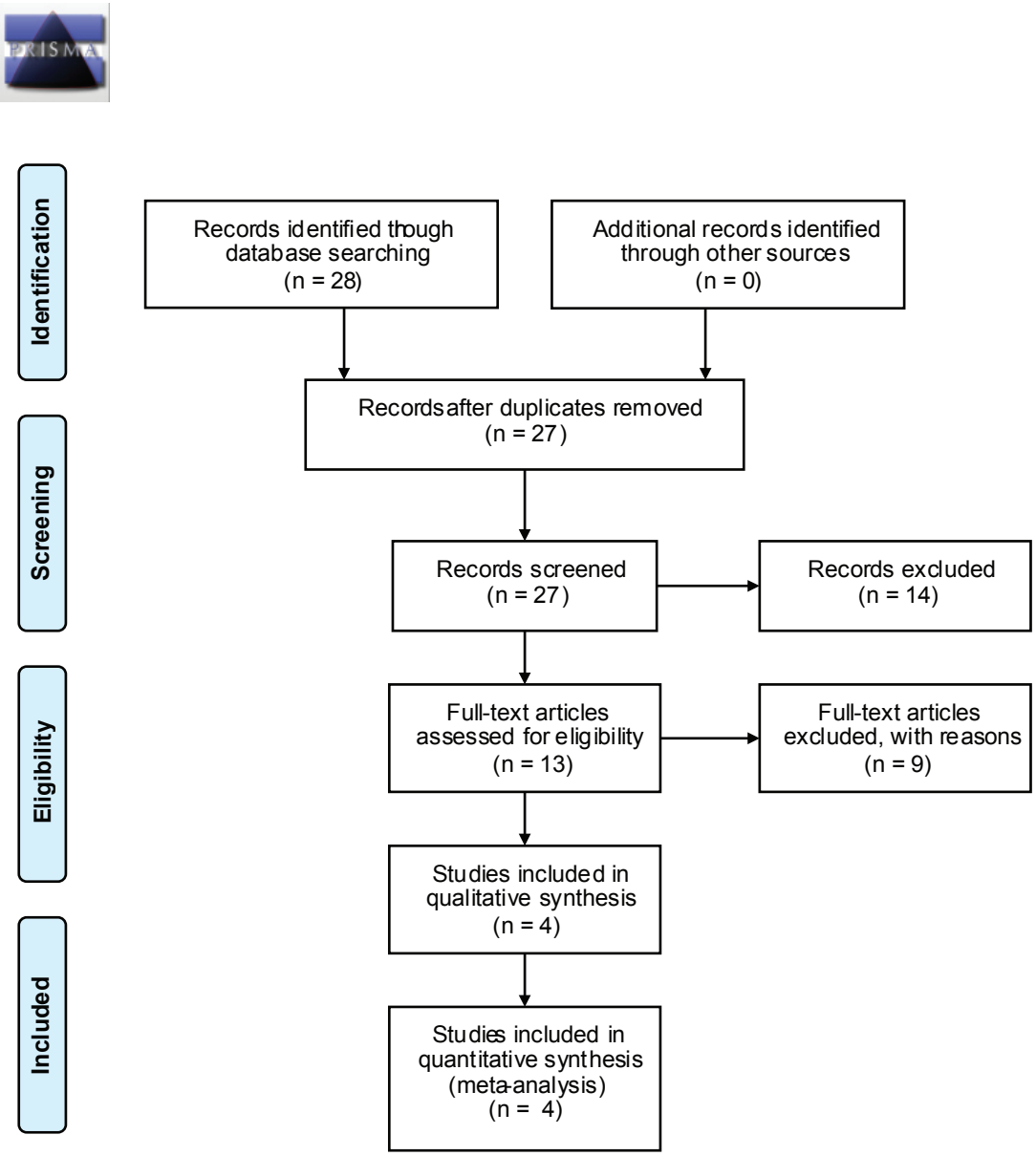

B) **MAD-AD Datasets**

Author	Database ID	Patients	Paired (LS/NL)	ChipID
Beck et al. 2014	GSE59294	16	7	GPL570
Khattri et al. 2014	GSE58558	19	16	GPL570
Gittler et al. 2012	GSE36842	7	7	GPL570
Suárez-Fariñas et al. 2011	GSE32924	14	11	GPL570
Total		56	41	

C) **Meta-Analysis Workflow**

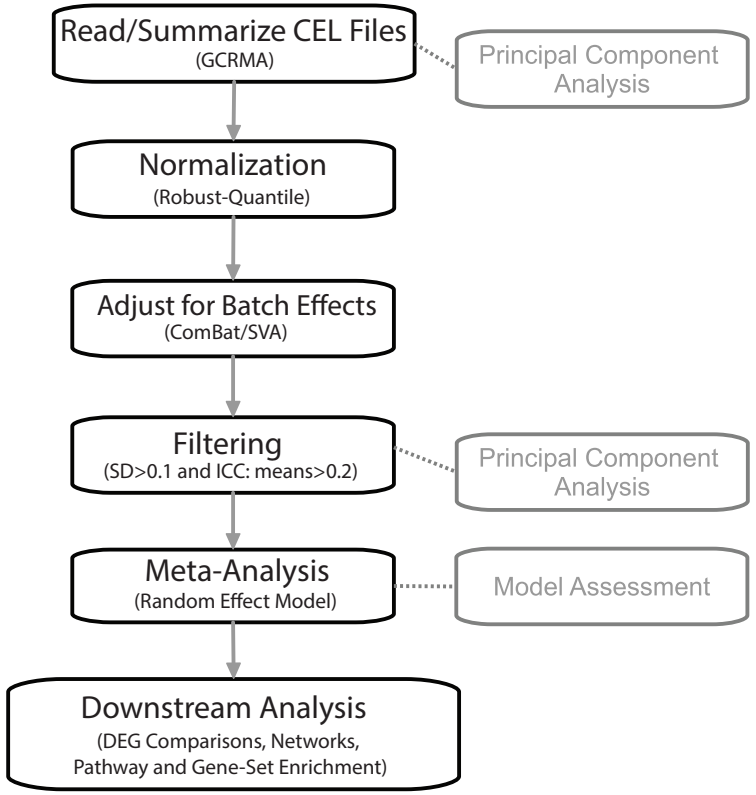

	GPL570
	GPL9052
	A-MEXP-1171
	GPL2700
	A-AFFY-141
	GPL570
	GPL96
sample size	
less genes)	GPL96, GPL97
ed in GSE32924	GPL570
ave	GPL6947
s, and two thirds of them treatet	
only LS	
expression in vitro)	
BDK vs. NHEK	
Flp-In HEK cells) treatet	
laCaT cells) treatet	
idermal keratinocytes (NHEK), treated	GPL6480
d qRT-PCR, No NL	GPL17344
aCaT keratinocytes)	
al human skin tissues	
atients (PSO+AD)	GPL14550
atitis	GPL570
itis	
licly available data of mouse and humans	

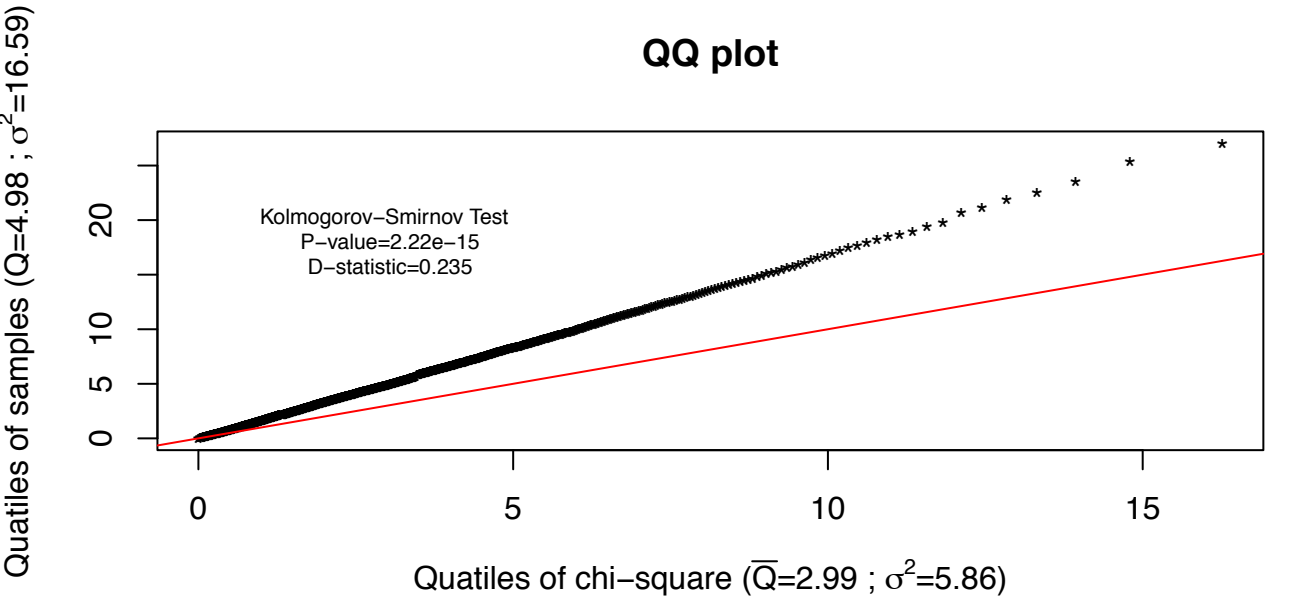
QQ plot
Kolmogorov−Smirnov Test
P−value=2.22e−15
D−statistic=0.235
Quatiles of samples (Q=4.98 ; σ2=16.59)
Quatiles of chi−square (Q=2.99 ; σ2=5.86)
0
5
10
15
20

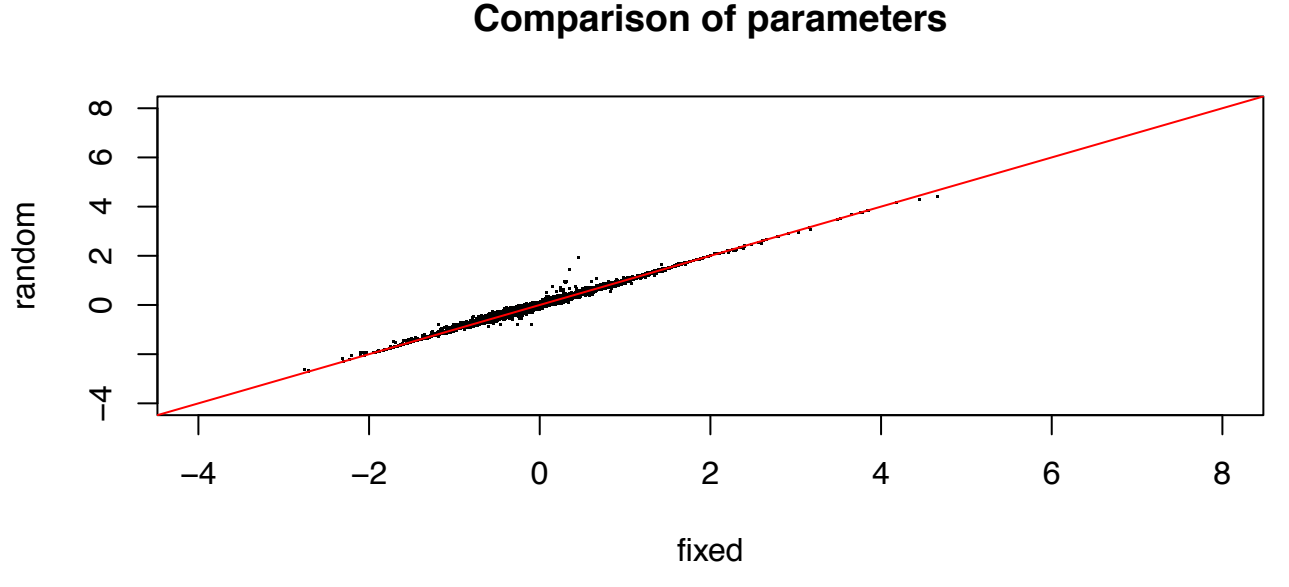
Comparison of parameters
random
fixed
−4
−2
0
2
4
6
8

Figure E3

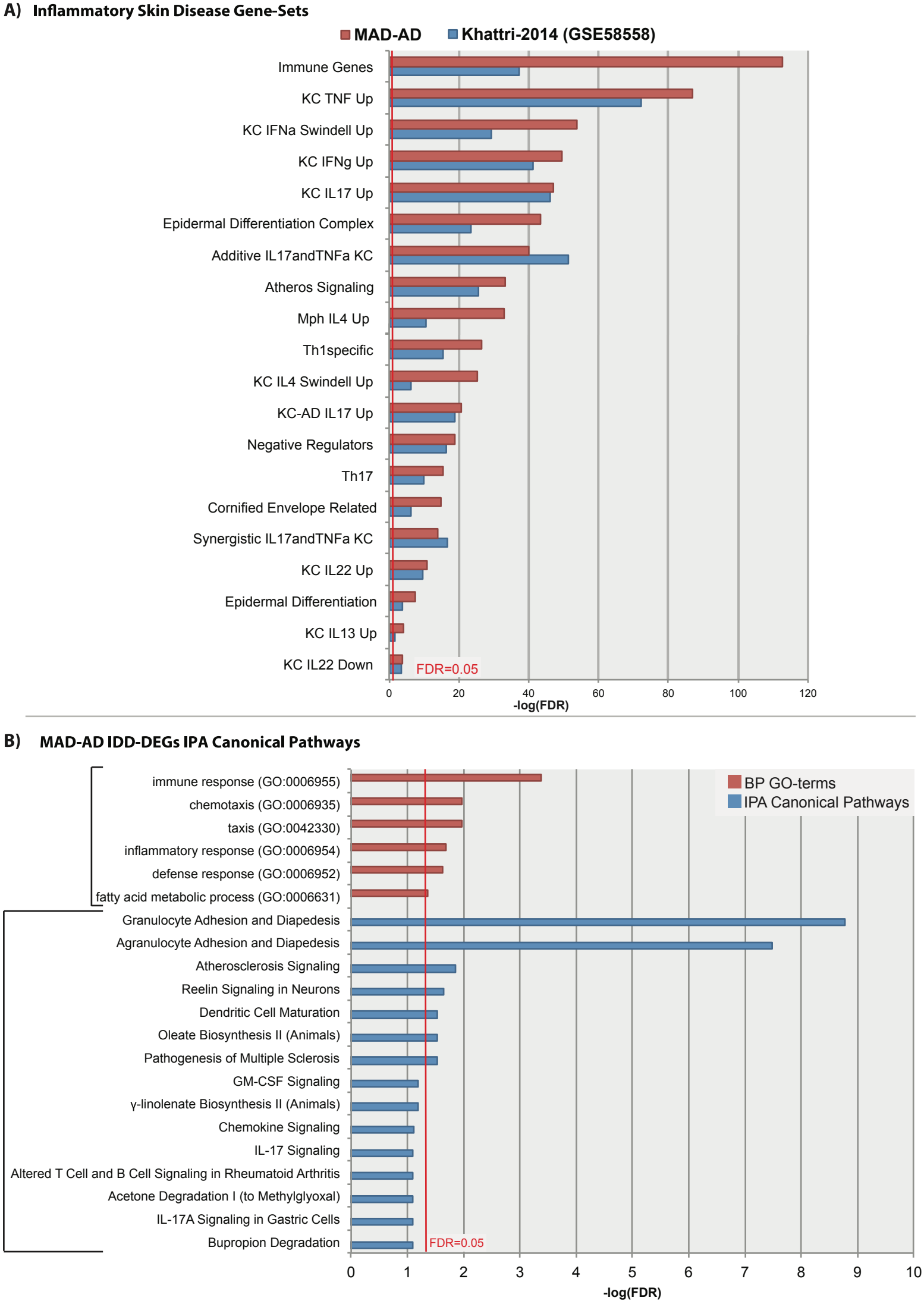
A) Inflammatory Skin Disease Gene-Sets
MAD-AD
Khattri-2014 (GSE58558)
Immune Genes
KC TNF Up
KC IFNa Swindell Up
KC IFNg Up
KC IL17 Up
Epidermal Differentiation Complex
Additive IL17andTNFa KC
Atheros Signaling
Mph IL4 Up
Th1specific
KC IL4 Swindell Up
KC-AD IL17 Up
Negative Regulators
Th17
Cornified Envelope Related
Synergistic IL17andTNFa KC
KC IL22 Up
Epidermal Differentiation
KC IL13 Up
KC IL22 Down
FDR=0.05
0
20
40
60
80
100
120
-log(FDR)
B) MAD-AD IDD-DEGs IPA Canonical Pathways
BP GO-terms
IPA Canonical Pathways
immune response (GO:0006955)
chemotaxis (GO:0006935)
taxis (GO:0042330)
inflammatory response (GO:0006954)
defense response (GO:0006952)
fatty acid metabolic process (GO:0006631)
Granulocyte Adhesion and Diapedesis
Agranulocyte Adhesion and Diapedesis
Atherosclerosis Signaling
Reelin Signaling in Neurons
Dendritic Cell Maturation
Oleate Biosynthesis II (Animals)
Pathogenesis of Multiple Sclerosis
GM-CSF Signaling
γ-linolenate Biosynthesis II (Animals)
Chemokine Signaling
IL-17 Signaling
Altered T Cell and B Cell Signaling in Rheumatoid Arthritis
Acetone Degradation I (to Methylglyoxal)
IL-17A Signaling in Gastric Cells
Bupropion Degradation
FDR=0.05
0
1
2
3
4
5
6
7
8
9
10
-log(FDR)

A)

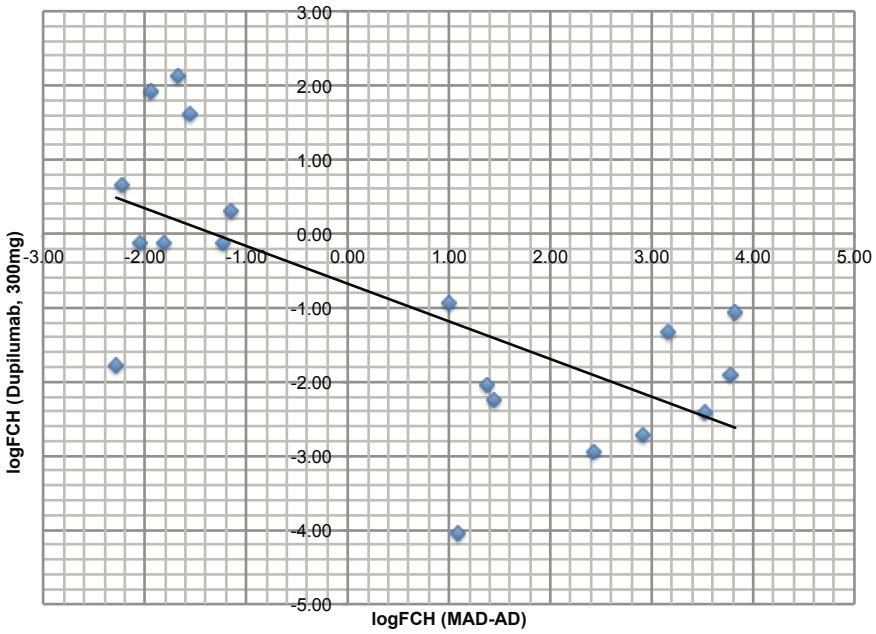
3.00
2.00
1.00
0.00
-1.00
-2.00
-3.00
-4.00
-5.00
-3.00
-2.00
-1.00
0.00
1.00
2.00
3.00
4.00
5.00
logFCH (Dupilumab, 300mg)
logFCH (MAD-AD)

B)

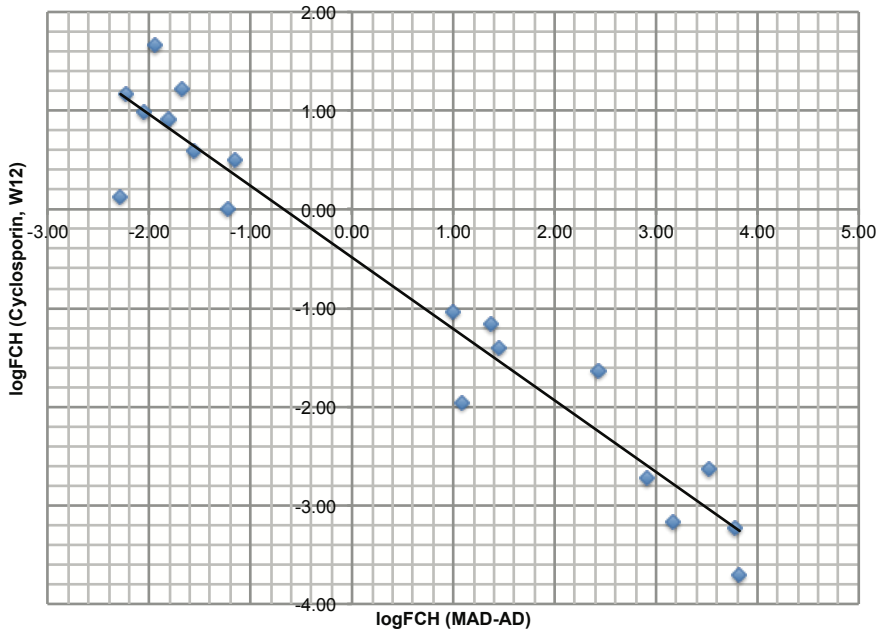
2.00
1.00
0.00
-1.00
-2.00
-3.00
-4.00
-3.00
-2.00
-1.00
0.00
1.00
2.00
3.00
4.00
5.00
logFCH (Cyclosporin, W12)
logFCH (MAD-AD)

C)

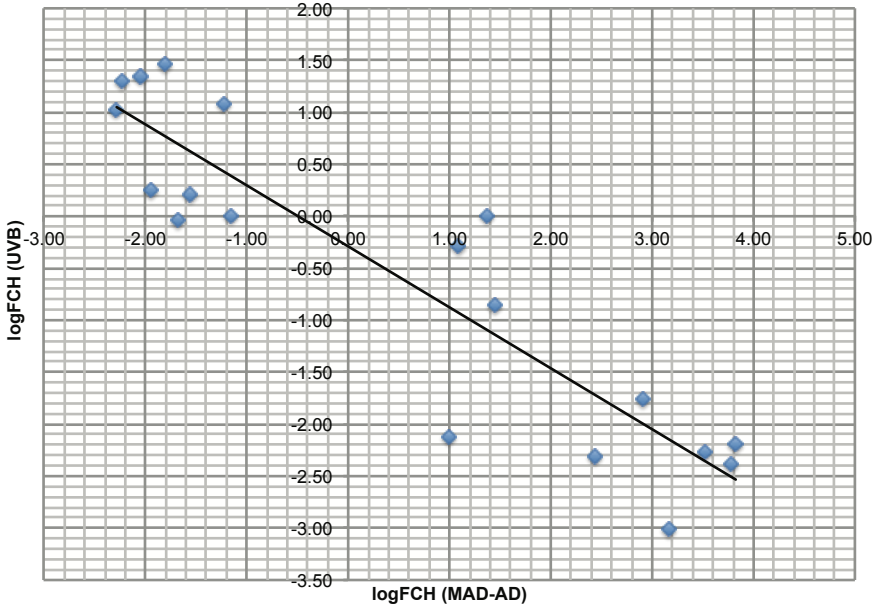
2.00
1.50
1.00
0.50
0.00
-0.50
-1.00
-1.50
-2.00
-2.50
-3.00
-3.50
-3.00
-2.00
-1.00
0.00
1.00
2.00
3.00
4.00
5.00
logFCH (UVB)
logFCH (MAD-AD)